NOVEMBER 1975 MATT-1172

HIGH FREQUENCY PARAMETRIC WAVE PHENOMENA AND PLASMA HEATING: A REVIEW

BY

M. PORKOLAB

PLASMA PHYSICS LABORATORY

PRINCETON UNIVERSITY
PRINCETON, NEW JERSEY

This work was supported by U. S. Energy Research and Development Administration Contract E(11-1)-3073. Reproduction, translation, publication, use and disposal, in whole or in part, by or for the United States Government is permitted.

DISCLAIMER

NOTICE

Printed in the United States of America.

Available from
National Technical Information Service
U. S. Department of Commerce
5285 Port Royal Road
Springfield, Virginia 22151
Price: Printed Copy $ *; Microfiche $1.45

*Pages	NTIS Selling Price
1-50	$ 4.00
51-150	5.45
151-325	7.60
326-500	10.60
501-1000	13.60

HIGH FREQUENCY PARAMETRIC WAVE PHENOMENA AND PLASMA HEATING: A REVIEW *

M. Porkolab

Princeton University Plasma Physics Laboratory

Princeton, New Jersey

ABSTRACT

A survey of parametric instabilities in plasma, and associated particle heating, is presented. A brief summary of linear theory is given. The physical mechanism of decay instability, the purely growing mode (oscillating two-stream instability) and soliton and density cavity formation is presented. Effects of density gradients are discussed. Possible nonlinear saturation mechanisms are pointed out. Experimental evidence for the existence of parametric instabilities in both unmagnetized and magnetized plasmas is reviewed in some detail. Experimental observation of plasma heating associated with the presence of parametric instabilities is demonstrated by a number of examples. Possible application of these phenomena to heating of pellets by lasers and heating of magnetically confined fusion plasmas by high power microwave sources is discussed.

1. INTRODUCTION

Under the influence of high frequency electromagnetic fields various modes of oscillation in the plasma may become coupled, and may grow exponentially in time or space before saturating at large amplitudes. For example, in the absence of a magnetic field electron plasma waves and ion acoustic waves may couple in such a manner

*Paper presented at Twelfth International Conference on Phenomena in Ionized Gases, Eindhoven, The Netherlands, August 18-22, 1975

(Dubois et al, Silin, Jackson, Nishikawa).[1]

If the incident electromagnetic wave ("pump wave") has a relatively long wavelength as compared with the wavelengths of the decay waves, then it is possible that energy is transferred to the particles via collective effects; namely, the energy transferred to the short wavelength decay waves from the pump wave is absorbed by particles more efficiently than the energy transferred to particles directly from the weakly damped pump wave. Thus, the net effect of this process is an "anomalous" absorption of the incident electromagnetic wave. This process is somewhat similar to turbulent heating, and it is expected to be of importance in hot plasmas where collisional absorption of electromagnetic energy is rather inefficient (Kaw and Dawson[2]). Nonlinear absorption should be distinguished from the process of linear mode conversion, in which efficient absorption of energy may occur only in a narrow critical layer (and only if the incident wave is not at normal incidence to an inhomogeneous plasma layer; Piliya[3]). Thus, parametric instabilities(which, however,have a finite threshold of pump power) may form a channel for efficient transfer of electromagnetic energy into rather large size hot plasmas. Because of its practical importance, this phenomena has been the subject of extensive investigation both theoretically and experimentally. In this paper we shall outline the fundamental aspects of this problem, and give a number of illustrations from the published (or to be published) literature.

We note that in a number of papers the coupling among different electrostatic waves of comparable wave-numbers have been studied in considerable detail. These processes, which form the foundations of weak turbulence theory, may be called more appropriately mode-mode

(or wave-wave) coupling. Instabilities due to these processes, which have been called decay instabilities, are akin to parametric instabilities as long as one of the waves is coherent in phase and large in amplitude as compared with other waves (Galeev and Sagdeev[4]). In fact, decay instabilities have been studied prior to the so-called "parametric" instabilities (Galeev and Sagdeev[4]). Thus, the naming of these processes is somewhat arbitrary, and indeed they have been often used interchangeably in the literature. We remark, however, that there are some decay instabilities which exist only if the pump has a finite wave-number. In the present paper we shall use the term "parametric instabilities" mainly to describe wave coupling phenomena in which the pump wave-number can be ignored as compared with the wave-number of the decay waves (although we shall give a few experimental references where this is not true). Thus, the pump can be either an electromagnetic wave or a long wavelength electrostatic wave. In the later case the thresholds and growth rates are nearly identical to those associated with an electromagnetic wave if the identification $\underset{\sim}{k}_o\phi_o = \underset{\sim}{E}_o$ is made (where k_o and ϕ_o are the wave-number and electrostatic pump potential, respectively, and $\underset{\sim}{E}_o$ is the pump electric field). An exception to this terminology are the various electromagnetic decay instabilities in which case at least two electromagnetic waves are involved in the decay process. We shall mention only briefly these in the theoretical section, and only one experimental example will be given.

The content of this paper will be organized as follows: In Section II a summary of linear parametric theory is given. Physically transparent concepts will be emphasized. In Section III a summary of nonlinear effects will be given, and the derivation of soliton

formation is presented. In Section IV a number of experiments will be discussed which illustrate the predictions of theory. Experimental results showing that plasma heating is associated with the excitation of parametric instabilities will be presented. In Section V the summary and conclusions are given.

2. LINEAR THEORY OF PARAMETRIC INSTABILITIES.

2.1. The Paramatric Decay Instability

In the presence of an rf electric field different species of particles (i.e., ions, electrons) are displaced relative to each other due to their different masses, thus causing monentary charge separation (Kruer and Dawson,[5] Nishikawa[1].) For example, in the absence of a magnetic field in a singly charged electron-ion plasma for rf pump frequencies $\omega_o \simeq \omega_{pe}$ (where ω_{pe} is the electron plasma frequency) the electrons make relatively large excursion in the electric field $E_o \cos\omega_o t$, i.e.,

$$\Delta x \simeq \frac{eE_o}{m_e\omega_o^2} \cos\omega_o t \quad , \qquad (1)$$

whereas the ions remain nearly stationary due to their large mass. If there are low frequency ion fluctuations in the background with frequency $\omega_1 \lesssim \omega_{pi}$ (where ω_{pi} is the ion plasma frequency) these may beat with the oscillating electrons to form additional oscillations in the charge at the frequency $(\omega_o \pm \omega_1)$, i.e.,

$$\delta n_e \simeq \frac{\partial n_i}{\partial x} \Delta x = ikn_i \frac{eE_o}{m\omega_o^2} \cos\omega_o t \quad . \qquad (2)$$

The spectrum of this process is shown schematically in Fig. 1.

The selection rules associated with this process are

$$\omega_o(\underset{\sim}{k}_o) = \omega_1(\underset{\sim}{k}_1) + \omega_2(\underset{\sim}{k}_2) \qquad (3)$$

$$\underset{\sim}{k}_o = \underset{\sim}{k}_1 + \underset{\sim}{k}_2$$

which is the usual resonant mode-mode coupling process, demonstrating energy and momentum conservation (Davidson[6]). For parametric instabilities we take $\underset{\sim}{k}_o \simeq 0$, and thus $\underset{\sim}{k}_1 \simeq -\underset{\sim}{k}_2$. (So that $|\underset{\sim}{k}_1| = |\underset{\sim}{k}_2| \equiv k$). Combining Eq. (2) with a simple harmonic oscillator equation which describes electron plasma waves, we obtain

$$\frac{\partial^2 n_e}{\partial t^2} + \nu_e \frac{\partial n_e}{\partial t} + \omega_{ek}^2 n_e = -\frac{\partial^2(\delta n_e)}{\partial t^2} = \frac{ikn_i eE_o}{m}\cos\omega_o t \qquad (4)$$

where $\omega_2 = \omega_{ek}$ is the resonance frequency of electron plasma waves in the absence of the pump field, and $\gamma_e = \nu_e/2$ is their linear damping rate. In the absence of a magnetic field

$$\omega_{ek}^2 = \omega_{pe}^2 + 3k^2 v_{te}^2$$

is the Bohm-Gross dispersion relation (where $\omega_{pe} = (4\pi ne^2/m)^{1/2}$ is the electron plasma frequency, $v_{te} = (T_e/m_e)^{1/2}$ is the electron thermal speed, and T_e is measured in units of energy). We also assumed that the displacement given by Eq. (1) is small as compared with a typical wavelength (i.e., k_1^{-1}). This, plus the fact that only ω_2 is near a resonant frequency justifies ignoring coupling to other harmonics (the case of strong coupling has been discussed by Silin[1].)

Consider now the reverse of this process, namely the beating of the electron plasma wave with the rf pump field. This beat produces a ponderomotive force which exerts additional pressure on electrons at low frequencies:

$$\nabla\delta p = \nabla\left(\frac{E^2}{8\pi}\right) = \frac{E_o}{4\pi}\frac{\partial E}{\partial x}\cos\omega_o t = -eE_o\delta n_e\cos\omega_o t \qquad (5)$$

where we made use of Poisson's equation. Note that the ponderomotive force is equivalent to the $\underset{\sim}{v}\cdot\nabla_x\underset{\sim}{v}$ term, since

$$v_x\frac{\partial v_x}{\partial x} = \frac{1}{2}\frac{\partial}{\partial x}(v_x^2) = \frac{1}{2}\frac{\partial}{\partial x}\frac{e^2E^2}{m^2\omega_o^2} \quad ,$$

and using $\omega_o^2 \simeq \omega_{pe}^2 = 4\pi ne^2/m_e$ we obtain

$$nm_e v_x\frac{\partial_x v_x}{\partial x} = n\nabla_x\left(\frac{E^2}{8\pi n}\right) \quad .$$

Thus, considering that ion acoustic waves are driven by electron pressure, namely $\omega_l \simeq \omega_s$ where

$$\omega_s^2 n_i = \frac{k_l^2 Tn_i}{m_i} = \frac{k^2(p+\delta p)}{m_i} \quad , \qquad (6)$$

the simple harmonic oscillator equation for ions becomes

$$\frac{\partial^2 n_i}{\partial t^2} + \nu_s\frac{\partial n_i}{\partial t} + \omega_s^2 n_i = -\frac{ikenE_o}{m_i}\cos\omega_o t \qquad (7)$$

where we included Eq. (5) for δp, and where $\nu_s/2 = \gamma_s$ is the linear damping rate of ion acoustic waves. Thus, we see that

Eqs. (4) and (7) represent the coupled oscillator equations for short wavelength ion and electron waves in the presence of the long wavelength rf pump wave. Solving Eqs. (4) and (7) by Fourier transformation, we find that if the selection rules Eq. (3) are obeyed then both electron and ion waves grow exponentially in time above the threshold field

$$\frac{\gamma_e \gamma_s}{\omega_{ek} \omega_s} < \frac{E_o^2}{64\pi n_o T_e} \quad , \tag{8}$$

and that well above threshold the growth rate γ is obtained from Eq. (8) by replacing $\gamma_e \gamma_s = \gamma^2$. We note the following: a). A minimum threshold exists since there are linear losses present initially which the pump wave has to overcome; b) In order to obtain Eq. (8) we assumed $\omega_s > \gamma_e$ so we could ignore the upper sideband $(\omega_o + \omega_s)$ (or anti-Stokes line).

2.2. The Purely Growing Mode.

Nishikawa[5] showed that in the limit $\omega_1 \to 0$, at $k \neq 0$ another instability may also occur, which is called the "purely growing mode" or the "oscillating two stream" instability. In particular, by Fourier analyzing Eqs. (4) and (7), and retaining both sidebands $\omega_{ek} \sim (\omega_o \pm \omega_1)$, for $\mathrm{Re}\ \omega_1 = 0$ we obtain the following threshold:

$$\frac{\gamma_e}{\omega_o} < \frac{E_o^2}{32\pi n_o T_e} \tag{9}$$

For weakly damped modes ($T_e >> T_i$), $\gamma_s/\omega_s << 1$, and the threshold for the purely growing mode is higher than that of the decay instability. We note that if we include a finite k_o, the purely growing mode assumes finite real frequencies. An alternate way to derive the purely growing mode will be indicated in the next section, where we show that it is the linearized limit of the so-called nonlinear-Schrodinger equation which predicts solitons.

In the presence of a magnetic field the situation becomes much more complicated than that shown above. For example, if we assume a dc magnetic field in the $\hat{z}$ direction, and an external electric field of the form

$$\underset{\sim}{E}_o(\underset{\sim}{x},t) = (E_{ox}\hat{x} + E_{oz}\hat{z})\cos\omega_o t \quad , \qquad (10)$$

electrons are displaced relatively to ions according the relations:

$$\Delta x = \frac{e}{m}\frac{E_{ox}\cos\omega_o t}{\omega_o^2 - \Omega^2} \qquad 11(a)$$

$$\Delta y = \frac{\Omega}{\omega_o}\frac{e}{m}\frac{E_{ox}\sin\omega_o t}{\omega_o^2 - \Omega^2} \qquad 11(b)$$

$$\Delta z = \frac{e}{m}\frac{E_{oz}\cos\omega_o t}{\omega_o^2} \qquad 11(c)$$

where $\Omega = eB/mc$ is the electron cyclotron frequency. Since the oscillating particles may couple with waves with wave vectors $\underset{\sim}{k}$ (so that the driving term of the instability is $\underset{\sim}{k} \cdot \underset{\sim}{\Delta x}$) we see that waves which propagate parallel to the magnetic field are driven

by the $k_{\parallel}\Delta z$ term, whereas waves propagating mainly perpendicularly to the magnetic field are driven by the term $\underset{\sim}{k}_{\perp}\cdot\Delta\underset{\sim}{x}_{\perp}$. A unified treatment of the problem of parametric coupling of waves in a magnetic field has been considered by Aliev et al,[7] Amano and Okamoto,[8] Porkolab,[9,10] etc. These authors used the Vlasov equation, which can be solved easily after transformation to the oscillating frame of reference. The resulting dispersion relation in the limit of weak coupling can be written in the following form:

$$\varepsilon(\omega) + \frac{\mu^2}{4}\chi_i(\omega)[1+\chi_e(\omega)]\left[\frac{1}{\varepsilon(\omega-\omega_o)} + \frac{1}{\varepsilon(\omega+\omega_o)}\right] = 0 \qquad (12)$$

where we assumed $\varepsilon(\omega-\omega_o)<<1$. Here

$$\varepsilon(\omega \pm j\omega_o) = 1 + \chi_i(\omega \pm j\omega_o) + \chi_e(\omega \pm j\omega_o) ,$$

is the linear dielectric function, $j = 0, \pm 1$, and $\chi_i(\chi_e)$ is the linear ion (electron) susceptibility. These susceptibilities can be written quite generally in terms of the complete hot plasma dielectric tensor in a magnetic field, including collisions. The coupling coefficient μ is given by the expression

$$\mu = \frac{e}{m}\left[\left(\frac{E_{o\parallel}k_z}{\omega_o^2} + \frac{E_{ox}k_x+E_{oy}k_y}{\omega_o^2-\Omega^2}\right)^2 + \frac{(E_{ox}k_y-E_{oy}k_x)^2\Omega^2}{(\omega_o^2-\Omega^2)^2\omega_o^2}\right] \qquad (13)$$

which shows the effects of parallel drift, perpendicular polorization drift, and $\underset{\sim}{E}\times\underset{\sim}{B}$ drift.

In the limit of weakly damped waves Eq. (12) can be expanded about the low and high frequency normal modes ω_1 and ω_2, respectively, and we obtain for the growth rate γ,

$$(\gamma+\gamma_1)(\gamma+\gamma_2) = -\frac{\mu^2\chi_i(\omega_1)(1+\chi_e(\omega_1)}{4\frac{\partial\varepsilon_1}{\partial\omega}\Big|_{\omega_1}\frac{\partial\varepsilon_2}{\partial\omega}\Big|_{\omega_2}} \qquad (14)$$

where we neglected the upper sideband. Here γ_1, γ_2 are the linear damping rates, and

$$\mathrm{Re}\varepsilon_j(\omega_j,k_j) \approx 0$$

define the normal modes $\omega_j(k_j)$, $j = 1, 2$. We note that these normal modes satisfy the selection rules Eq.(3). The threshold is obtained from Eq.(14)by setting $\gamma = 0$. Similarly, by letting $\mathrm{Re}\omega_1 = 0$, and keeping both lower and upper sidebands $\varepsilon(\omega \pm \omega_o)$, we can obtain the purely growing mode (Porkolab[9]). Using Eq.(14), the thresholds for a number of different modes in a magnetized plasma have been obtained (Porkolab[9,10,11]).

In Fig. 2 we show schematically different modes in a magnetized plasma which may be used as pump waves and/or decay waves. In Table 1 we present various combinations of these modes which may form triplets of decay waves which have been considered and/or observed in recent experiments.

There are also more complicated processes than the simple cases discussed in the foregoing paragraphs. For example, the decay of a whistler wave into another whistler wave and an ion acoustic wave is an example of the so-called Brillouin scattering, in which an incident electromagnetic wave decays into another electromagnetic wave and an ion acoustic wave (Forslund et al[12], Porkolab et al[13]).

In this case the coupling mechanism is the $\underset{\sim}{j} \times \underset{\sim}{B}$ force, i.e., particles oscillating in the electric field of one of the wave produce a current $\underset{\sim}{j}$, which then couples with the magnetic field component $\underset{\sim}{B}$ of the second EM wave. The $\underset{\sim}{j} \times \underset{\sim}{B}$ force then gives a contribution to electron pressure which may drive electrostatic ion waves unstable. This process is of the back-scatter-type, namely,

$$\underset{\sim}{k}_o = -\underset{\sim}{k}_1 , \qquad \underset{\sim}{k}_2 = 2\underset{\sim}{k}_o \tag{15}$$

where $\underset{\sim}{k}_2$ is the wave vector of the ion wave. This type of instability may also occur in the absence of a magnetic field, and in laser fusion schemes it could be dangerous and undesirable. In particular, if a large fraction of the incident power were reflected from the outer layers of the expanding plasma, it would reduce efficiency and/or damage optics (Forslund et al[14], Eidman and Sigel[15]).

There are other types of decay processes which may be of importance in laser fusion. A schematic of some processes of interest is shown in Fig. (3). In particular, noteworthy processes include the Raman-scatter (EM → EM + E.P.), decay into two electron plasma waves (EM → E.P. + E.P.), Compton (induced) scatter (EM → EM + Particles), and filamentational and modulational instabilities (where EM designates the electromagnetic wave, and E.P. designates longitudinal electron plasma waves). Thresholds and growth rates for these processes have been given in the literature (see, for example, DuBois[16], Drake et al[17], Manheimer and Ott[18]). Since to present date experimental evidence for the existence of these instabilities are rather lacking, and since the subject of laser-fusion related phenomena

is very extensive, we shall refer the reader to the excellent review article of DuBois[16].

One final case of interest in Table 1 is the decay of the slow (lower-hybrid) wave and/or whistler wave into short wavelength lower-hybrid waves and ion quasi-modes. This process is akin to induced Compton scatter (or nonlinear Landau damping) and is expected to be of importance in rf heating of confined thermonuclear fusion plasmas (Porkolab[10]). In this process the beat of two weakly damped lower-hybrid waves may resonate with electrons and/or ions, thus heating the bulk of particles. The selection rules for this process are

$$(\omega_o - \omega_e)/k_\parallel \simeq v_{te} \qquad 16(a)$$

or

$$\frac{(\omega_o - \omega_e)}{k_\parallel} \simeq n\Omega_i/k_\parallel \simeq v_{ti} \quad . \qquad 16(b)$$

Although according to the Manley-Row relations (Louisell[19])

$$\frac{P_s}{\omega_s} = \frac{P_e}{\omega_e}$$

(where P_j is the power density carried by each wave) most of the power flow is into the high frequency wave, due to the long confinement times of present and future tokamaks, and to the relatively large growth rates, considerable ion heating may be expected. This nonresonant process is sometime also called "resistive quasi-mode". At large pump powers ($E^2/4\pi nT \simeq 1$) two other nonresonant processes may occur, namely decay into "reactive" (or fluid)

quasi modes (Nishikawa[5], Porkolab[10], Drake[17] et al), and the "kinetic" instability (Silin[20]).

2.3. Convective Effects due to Inhomogeneities.

In recent years considerable effort has been spent on taking into account the effects of inhomogeneities of density, temperature, finite interaction region, and nonuniform pump effects. (Kroll[21], Porkolab et al[22], Harker et al[23], Perkins et al[24], Rosenbluth et al[25], Pesme et al[26], Liu et al[27], DuBois et al[28], Forslund et al[29]). All of these processes may introduce new, possibly higher than uniform plasma thresholds for instability. The essential feature of these effects is that often the instabilities become convective (forward scatter) and the matching of the selection rules (Eq. 3) is destroyed in a distance short compared with effective growth lengths. Alternatively, finite lengths or nonuniform pumps limit the region of spatial growth. However, for backward scatter $(\underset{\sim}{v}_1 \cdot \underset{\sim}{v}_2 < 0)$ absolute instability may occur if

$$\gamma_o^2 > \frac{|v_1 v_2|}{4}\left(\frac{\gamma_1}{v_1} - \frac{\gamma_2}{v_2}\right)^2 \qquad (17)$$

where v_1, v_2 are the group velocities of the two decay waves, γ_1, γ_2 are their damping rates, and γ is the homogeneous, uniform plasma growth rate (See for example, Pesme et al[26]).

The effects of density gradients can be obtained following the procedure outlined by Rosenbluth[25]. Assuming a WKB type phase variation and defining

$$K(X) = \Delta K = k_o - k_1 - k_2$$

(where we assumed a one-dimensional propagation so that all k's depend on x only) the equations describing the spatial variation of the two coupled modes can be written in the following form (Rosenbluth[25]):

$$\frac{dE_1}{dx} + \frac{\gamma_1}{v_{1x}} E_1 = \frac{\gamma E_2^*}{v_{1x}} \exp(i \int_o^x K(x)dx) \qquad 18(a)$$

$$\frac{dE_2}{dx} + \frac{\gamma_2}{v_{2x}} E_2 = \frac{\gamma E_1^*}{v_{2x}} \exp(-i \int_o^x K(x)dx) \qquad 18(b)$$

where E_1, E_2 are the electric field amplitudes of the decay waves, and the other quantities have been defined earlier.

Assuming a linear variation of the mismatch with distance, namely $K(x) \simeq K'x$, Eqs. 18(a) and 18(b) can be combined in the following form:

$$\frac{d^2\psi}{dx^2} - [\frac{\zeta^2}{4} + \frac{1}{2}\frac{d\zeta}{dx} + \frac{\gamma_o^2}{v_1 v_2}]\psi = 0 \qquad 18(c)$$

where $\zeta = \gamma_2/v_{2x} - \gamma_1/v_{1x} - iK(x)$, and $\psi \propto E_1$. Integrating Eq. (18) by WKB techniques, the total spatial amplification of wave intensity obtained between the turning points $x_t = 2\gamma_o/K'(v_{1x}v_{2x})^{1/2}$ is given by

$$I = I_o \exp\left(\frac{2\pi\gamma_o^2}{|K'|v_{1x}v_{2x}}\right) \qquad (19)$$

(where linear damping has been ignored). Thus, the effective threshold defined as the pump power for which a factor of 2π e-folding of the initial background noise results is

$$1 < \frac{\gamma_o^2}{|K'|v_{1x}v_{2x}} \quad . \tag{20}$$

For example, for decay into ion acoustic waves and electron plasma waves

$$K'v_{1x}v_{2x} \simeq \frac{\partial \omega_p}{\partial x} c_s \left(\frac{k_x}{k}\right)^2 ,$$

so that the inhomogeneous threshold becomes

$$\frac{v_o^2}{v_t^2} > \frac{16k_x}{Hk^2} \quad , \tag{21}$$

where H is the density gradient scale length, $v_t = (T_e/m_e)$, $v_o = eE_o/(m\omega_o)$ is the rf drift velocity of electrons, and where we used $\gamma^2 = \omega_s\omega_p v_o^2/(16v_t^2)$ with $\omega_s = kc_s$ (See Eq. 8). In the case of weakly damped waves k_x assumes a minimum value when the WKB conditions break down, $k_x \simeq (\pi/x)$ so from the dispersion relation of electron plasma waves

$$\omega_{ek}^2 = \omega_{pe}^2(1 + x/H) + 3(k_x^2 + k_z^2)v_{te}^2 \tag{22}$$

we obtain $k_{xmin}^3 \simeq (H\lambda_D^2)^{-1}$ (where $\lambda_D = v_{te}/\omega_{pe}$ is the Debye length). Hence the threshold becomes

$$\frac{v_o^2}{v_t^2} > \frac{16}{(k^2\lambda_D^2)}\left(\frac{\lambda_D}{H}\right)^{4/3} . \tag{23}$$

The minimum value is obtained for the largest value of k just before strong Landau damping sets in at the sideband, namely $k\lambda_D \simeq 1/4$.

For strongly damped ion waves ($T_e \simeq T_i$) we have $k_{xmin} \simeq (\omega_1 \gamma_1)^{1/2}/c_s$ (Perkins and Flick,[24]) so that Eq. 21 becomes

$$\frac{v_o^2}{v_t^2} > \frac{16(\omega_1 \gamma_1)^{1/2}}{Hc_s k^2} = \frac{16}{Hk}\left(\frac{\gamma_1}{\omega_1}\right)^{1/2} \qquad (24)$$

where we used $\omega_1 \simeq c_s k$. Again the minimum threshold obtains at $k\lambda_D \sim 1/4$.

If the group velocities of the decay waves are in the opposite direction, and if $K' = 0$, but $K'' \neq 0$, then absolute instability may result (Rosenbluth[25]). On the other hand, if finite size effects are included, for $\underset{\sim}{v}_1 \cdot \underset{\sim}{v}_2 < 0$, the convective instability may become an absolute instability at the threshold given by Eq. 21 even if $K' \neq 0$. (DuBois et al[28]). According to Nicholson and Kaufman,[30] and Spatchek et al [31], if background turbulence is present absolute instability may result even in an inhomogeneous plasma. Finally, we note that the effect of a broad rf pump may reduce the growth rates considerably (Valeo and Oberman[32], Thomson[33]).

3. NONLINEAR EFFECTS AND SOLITON FORMATION

3.1. Nonlinear Effects

So far we have only considered linearized perturbation type solutions. An important question is the nonlinear limit of these instabilities. There have been several attempts to describe the nonlinear saturated state as being due to induced scattering and cascading of the sideband into further lower frequency waves (Pustovalov et al[34], Dubois et al[35], Valeo et al[36], Fejer et al[37], DuBois et al[38],), resonance broadening (Bezzerides et al[39]). Other possible mechanisms include pump depletion and quasi-linear effects (i.e., heating).

Associated with the decay instabilities one may define a nonlinear conductivity as follows (DuBois[16]):

$$\sigma_{NL}E_o^2 \equiv \frac{\nu_{eff}}{4\pi} E_o^2 = \int \frac{d^3k}{(2\pi)^3}[\gamma(E_o,k)-\gamma(0,k)]\frac{<|E_k|^2>}{4\pi} \qquad (25)$$

where the left hand side is the effective pump energy depletion rate, and the right hand side is the rate of growth of the energy of the excited electrostatic wave (where the negative contribution due to damping is subtracted). Note that by the above equation one could also define an effective "nonlinear resistivity," "ν_{eff}." In order to calculate the nonlinear conductivity, one has to have a theory for the saturated spectrum. This has been done only in a few special cases as mentioned above. For example, in the case of $T_e = T_i$, the nonlinear conductivity just above threshold was calculated by DuBois et al[38])

$$\sigma_{NL}(E_o) = \eta \frac{\omega_{pe} E_o^2}{16\pi n T_e} \qquad (26)$$

where η is a numerical coefficient of the order of unity. However, for large values of E_o the total energy goes as E_o^2 (instead E_o^4) so that σ_{NL} approaches a constant value, independent of E_o.

While the linear theory of parametric instabilities is now well understood (except in strongly inhomogeneous plasmas), with a few possible exceptions the nonlinear state is still not well understood. In addition, there are very few experimental results to verify these theories. Here computer simulation has been of considerable help and guidance (Kruer et al[40], Degroot et al[41], Thomson et al[42], Forslund et al[29]). However, how realistic these computer "experiments" are is still not known.

3.2. Soliton Formation and Density Cavities

Let us now consider another type of nonlinear solution, namely soliton formation. This may be relevant to the nonlinear state of the purely growing mode (Zakharov[43], Karpman[44], Morales et al[45], Valeo et al[46], Kaufman et al[47], Hasegawa[48]). In particular, due to the ponderomotive force, strong local electric fields may deplete the density, hence trapping the electric field. As the field grows more density is removed and a cavity is produced which then traps the fields further, etc., until possibly a collapse of the field occurs (at least in one dimension). Since locally strong fields may be produced, we may expect strong particle acceleration and energetic tail formation.

As shown by the above authors, the equation describing this nonlinear state is the nonlinear Schrodinger equation. It can be obtained as follows: Ignoring the magnetic field, and assuming $\omega_o \simeq \omega_{pe}$, the low frequency ($\omega \simeq 0$) time-averaged response of electrons in the presence of the external electric field is described by Eq. (5), namely we balance the pressure by the ponderomotive force:

$$\nabla_x p_e + \nabla_x \left(\frac{|E|^2}{8\pi}\right) = ne\nabla_x \phi \qquad (27)$$

where electron inertia is ignored, and where we included an ambipolar potential ϕ. Although only electrons respond to the ponderomotive force, ions respond to the ampipolar potential (trying to achieve charge neutrality):

$$\nabla_x p_i = -ne\nabla_x \phi \qquad (28)$$

where we ignored ion inertia. Requiring quasi-neutrality, namely $n_e \simeq n_i$, and since $p_e = n_e T_e$, $p_i = n_i T_i$, we may eliminate ϕ from Eqs. (27) and (28) and obtain

$$n(x) \simeq n_o \exp\{-[\frac{|\bar{E}|^2 - <|\bar{E}|^2>}{16\pi n(T_e+T_i)}]\} \tag{29}$$

where the bar represents time average, and $< >$ represents spatial average. Equation (29) describes modifications in the equilibrium density due to the high frequency field.

Let us now consider the high frequency response at the electron plasma frequency, $(\omega_o \simeq \omega_{pe})$ which is described by the simple harmonic oscillator motion:

$$\frac{\partial^2 E}{\partial t^2} + \omega_{ek}^2 E + \nu_e \frac{\partial E}{\partial t} = 0 \tag{30}$$

where we used the left hand side of Eq. (4), and used Poisson's equation, namely $E \propto n_e$ at high frequencies. Then recognizing that $\omega_{ek}^2 \simeq \omega_{pe}^2 + 3k^2\lambda_D^2$, and that $\omega_{pe}^2 \propto n(x)$, we may perform a WKB type expansion of E, namely assume $E = E_H(t,x)\exp(-i\omega_o t)$ (where E_H is a slowly varying function of x and t). From Eqs. (29), (30), and from the resonance condition $\omega_o^2 = \omega_{ek}^2(x = 0)$ we obtain

$$i\frac{\partial E_H}{\partial t} + \frac{3v_t^2}{2\omega_o}\frac{\partial^2 E_H}{\partial x^2} + \frac{\omega_{po}^2}{2\omega_o}\frac{|\bar{E}_H|^2}{16\pi n T_e} E_H = 0 \tag{31}$$

where $v_{te}^2 = T_e/m_e$, and where the last term of Eq. 31 contains the cubic nonlinearity. This is the so-called nonlinear Schrodinger equation. It is easy to show that in the linearized limit Eq. (31) predicts the purely growing mode. The computer solution of this

equation in the nonlinear limit has been discussed recently in some detail (Morales[45]). If we include ion inertia, a similar equation is obtained in the moving frame of reference, except the nonlinear term (the last term in Eq. 31) is divided by the term $(1 - v_g^2/c_s^2)$, where c_s is the speed of sound, and v_g is the group velocity of the high frequency wave (this is valid only as long as $v_g \neq c_s$). The solution of this equation in higher dimensions is still under present investigation. In particular, this equation may be unstable to transverse perturbations (Schmidt[49]).

4. EXPERIMENTAL OBSERVATIONS

4.1. Early Experiments

The early experimental work concerning parametric instabilities is summarized in Table II. This includes the works of Stein, Hiroe and Ikegami,[50] Chang and Porkolab[51,52], Stenzel and Wong[53], and Franklin et al[54]. In these experiments the decay spectrum as well as wave number selection rules (Chang and Porkolab[51,52]) were measured and compared with the theoretically predicted threshold fields. In Fig. 4 we show the experimental results of Chang et al[52] which demonstrates the selection rules, Eq. 3. Approximately the same time, Gekker and Sizukhin[55], and Batanov et al[56], attempted to demonstrate anomalous absorption due to parametric instabilities by injecting plasma in a waveguide from one end, and measuring the transmission (or reflection) coefficient of microwave power sent from the other end. In Fig. 5(a) we show a sketch of the experimental setup and the results of such measurements, indicating strong reduction in the reflection coefficient above some threshold. Although energetic particles were also detected in some of these experiments, no measurements were made to detect the presence of parametric instabili-

ties.Eubank[57] attempted to improve on this situation by shining microwave power onto a plasma column in both the ordinary and the extraordinary modes of propagation. He had a probe in the plasma which detected ion acoustic oscillations up to the ion plasma frequency, as well as grided probes (energy analyzer) which showed plasma heating. However,the threshold measurements and/or anomalous absorption measurements remained less clear since due to the low-rise time of the microwave pulses (milliseconds) strong ionization occured near the open ended waveguide.

There were also a series of experiments performed in Q-machines by Dreicer et al[58], and Chu and Hendel[59]. The geometry used in these experiments is shown in Fig. 5(b). In these experiments the plasma was placed in a high-Q rf cavity, and by measuring the Q of the cavity it was possible to observe an increase in the dissipation above some critical threshold input power level. In Fig. 6 we exhibit the results of Chu and Hendel[59] which show the increase of plasma rf resistivity (1/Q), increase of effective plasma heating (T/T_o determined from conductivity measurements), and growth of noise spectrum (picked up by a probe from within the cavity). Figure 7 indicates in the same experiments a break in the absorption curve when the input power is above threshold for parametric instability. In particular, it appears that in the unstable regime $P_{abs} \propto E^4$, and hence it was concluded that $\nu_{eff} \propto E_o^2$, in agreement with the nonlinear theories of Valeo et al[36] and DuBois et al[38]. However, in the more recent experiments of Flick[60] the input power was extended to higher levels, and the $P_{abs} \propto E^4$ law was not observed. In particular even near threshold Flick finds a faster variation of P_{abs} with E than the fourth power, and a slower variation well

above threshold. In addition, the cascading process assumed in the theories of DeBois et al[38], and Valeo et al[36], was not observed in the experiment. Flick proposed that pump depletion and random phase effects may be the relevant processes to explain his experiments.

We should also mention here the results of Demirkhanov et al[61] who observed parametric instability and heating due to a modulated current in the plasma and, the work of Vdovin[62], who observed anomalous heating of a tokamak plasma.

We must also include here the results of high-power radar modification experiments in the ionosphere (Utlaut and Cohen[63], Wong and Taylor[64], Carlson et al.[65]). These experiments also showed that parametric instabilities are operative and are responsible for some of the observed plasma heating in the ionosphere.

In Tables 3 and 4 we list some of the more recent experiments in which parametric instabilities and the resulting plasma heating were studied in more detail than previously. We shall now discuss these experiments in order of decreasing frequencies.

4.2. Upper-Hybrid Frequency

In the regime of the upper hybrid frequency recent measurements on parametric decay have been performed both in linear geometry (Grek and Porkolab[66]), Porkolab et al[67], and toroidal devices (Okabayashi et al[68]). These experiments include both the regime $\lambda_o << d$ and $\lambda_o >> d$ (where λ_o is the free-space wavelength of the electromagnetic wave, and d is the characteristic plasma size). Wavelength measurements of the decay waves showed decay into upper hybrid waves (Bernstein waves) and lower hybrid and/or ion acoustic waves. Measurements of thresholds, growth rates, pump depletion, and anomalous resistivity have been performed (Grek and Porkolab[66]).

It was shown that significant electron heating was associated with the presence of the decay instability. An effective anomalous resistivity of a factor of ten to twenty times larger than classical resistivity has been measured (Grek[66]). In Figs. 8 and 9 we show some of these experimental results on plasma heating. Significant heating was observed only above threshold for decay instability. Similar phenomena has been observed in the Princeton L-3 device (Porkolab et al[67]) and the Princeton FM-1 toroidal device (Okabayashi et al[68]). The results from the latter are shown in Figs. 10 and 11, again demonstrating that significant ion and electron heating occurs only above threshold for parametric instabilities. In this toroidal experiment in the presence of parametric instabilities no significant deterioration of confinement was observed. In particular, because of the short wavelengths excited ($k_\perp r_{ce} \simeq 1$) and decay well within the body of the plasma column, we do not expect much enhanced loss due to this instability. The localization of heating to the instability layer is shown in Fig. 12 (after

4.3. Electron Plasma Frequency.

Experiments showing parametric instabilities and plasma heating just above the electron plasma frequency have been performed recently by Dreicer et al[69], Mizuno and DeGroot[70], and Porkolab et al[67]. Dreicer's experiments were performed in a cavity geometry as discussed previously. Mizuno and DeGroot[70] made their measurements in a waveguide and an externally made plasma. In both of these experiments the resulting hot electron tail (suprathermal electrons) was measured. It was found that 1 to 10% of the particles ended up in the tail, depending on power and geometry (with Dreicer's experiments measuring the lower percentage). Maximum electron energies of up to two orders

of magnitude above thermal energy were detected for input powers up to three orders of magnitude above threshold.

In the experiments of Porkolab et al[67] a similar geometry was employed as that of Eubank (See Fig. 13), but the pulse rise-time was decreased to 50 nano-second, and the pulse duration was reduced to at most 10 μsecond so that ionization problems could be avoided. An attempt was made to verify the inhomogeneous threshold theory discussed earlier. However, it was found that while for some density profiles the spectrum behaved roughly in agreement with Eq. 23 (or 24) in many cases no such agreement was observed. In addition, the incident electric field was strongly nonuniform $[(\nabla n/n)^{-1} \sim (\nabla E/E)^{-1}$, so that the validity of the previous theories is in question. Also, strong refraction of the pump field around the plasma column was observed. In spite of the large gradients, strong parametric instabilities were observed near the critical layer ($\omega_o \simeq \omega_{pe}$) and plasma heating of the main body was observed above threshold. Although the incident power at threshold was higher than uniform theory predicted, because of the radially decreasing electric fields (similar to that shown in Fig. 12) the local electric field was estimated to be near the uniform threshold theory (within an experimental error of factor ~3). In Fig. 14 we show a typical low frequency decay spectrum (which was identified by interferometry as ion acoustic waves) and in Fig. 15 measurements of the heating rates of the main body electron temperature are shown. The heating results of Fig. 15 indicate an anomalous heating of a factor of twenty faster than classical collisional absorption. The production of energetic tails was also observed, with a few percent of the particles occupying the tail, and with maximum energies up to a factor of fifty above the mean bulk energy. In Fig. 16 we show a

distribution function for input powers two orders of magnitude above threshold. In addition, production of energetic ions was also observed (a few percent, with maximum energies up to 70 eV).

4.4. Trivelpiece-Gould Modes.

Because of possible applications to heat controlled fusion devices, a large number of experiments have been performed in this regime, i.e., $\omega_{pe} << \omega_o < \omega_{pe}, \Omega_e$, (Porkolab et al[71], Hendel and Flick[72], Flick[60], Chu et al[73], Bernabei et al[74], and Edgley et al[75]). In this regime decay into other Trivelpiece-Gould modes (or short wavelength electron plasma waves) and low frequency ion acoustic waves, or ion cyclotron waves, or ion quasi-modes occurs. We should also include here experiments using whistler waves (Porkolab et al[13]). In these experiments both energetic electron and ion tails have been observed at high input powers and short pulse times (Porkolab et al[13],) as well as main-body ion heating at longer times (Hendel et al[72]), Chu et al[73], Bernabei et al[74]). Examples of electron and ion tails (up to 10% of the particles) obtained in the regime $\omega_o \simeq (\omega_{ce}/2) \simeq (\omega_{pe}/10)$ are shown in Fig. 17, as well as the associated parametric decay spectrum. It is believed that the energetic ion tails are due to acceleration by the expanding parametrically heated energetic electrons, as well as due to the turbulent ion acoustic fields. In the work of Bernabei et al[74], main body ion heating was observed for pump frequencies $\omega_o \simeq 3\omega_{pi} << \omega_{pe}$, even though initially $T_{eo} >> T_{io}$. Simultaneously strong parametric decay spectrum in the ion cyclotron regime was observed as shown in Fig. 18. In Fig. 19 we show results obtained in a Q-machine ($T_e = T_i$) by Chu et al[73]. These authors operated in the regime $\omega_{pi} << \omega_o << \omega_{pe}$, and observed parametric decay in the ion cyclotron regime and concomitant main body ion

heating. In all of these cases significant heating was observed only above threshold for parametric excitation.

4.5. Lower Hybrid Waves.

There are several experiments in this regime ($1 < \omega_o/\omega_{LH} < 3$) which show parametric decay and strong heating (Farenik et al[77], Chang and Porkolab[78], and Brusati, et al[79]). In this regime decay into lower hybrid waves and ion acoustic waves, ion cyclotron waves, ion quasi modes, or drift waves may occur (Porkolab[9,10,11,80], Kindel et al[81], Berger et al[82], Karney et al[83], Rogister [84], Ott[85]). The purely growing mode has been demonstrated recently by Doppler shifting the frequency by a radial dc electric field, so as to produce a real part of the frequency ($\omega_k = kV_D$) in the laboratory frame of reference (Chang and Porkolab[78]). In Fig. 20 we domonstrate verification of the excitation of ion quasi-modes (after Chang and Porkolab[78]). In this experiment both parallel and perpendicular wavelengths of the decay waves were measured. In the same experiment strong plasma heating was observed above threshold for parametric instabilities (both ions and electrons). This is shown in Fig. 21. Note the increase of plasma heating as the lower hybrid frequency is approached (between 20 and 30 MHz). Brusati et al[79] observed similar effects.

We also note here the important high input power experiments done in this regime (Glagolev et al[86], Grigoreva et al[87], and Kitsenko et al[88]). In these experiments a few hundred kW's of rf power were applied for times of the order of 100 μsec. Ion and electron temperatures of the order of several hundred eV were observed. Again, we believe parametric instabilities may have been responsible for the plasma heating (although no experimental data

were obtained to identify such phenomena). One important question in applying these results to heating confined fusion plasmas will be possible excitation of drift waves, which may possibly lead to enhanced plasma loss (Sundaram and Kaw[89]). To present date no detailed experimental information related to this question is available.

4.6. Magnetosonic Waves.

These waves represent a contribution of the whistler wave branch in the regime $\omega_{ci} < \omega_o < \omega_{pi}$. A number of theoretical papers considered parametric decay instabilities in this regime (Ivanov and Parail[90], Sperling and Perkins[91], Kitsenko and Stepanov[92], Harms et al[93], and Martinov and Samain[94]). In addition, a number of experiments have been performed both in linear devices and in toroidal devices (Voloshko et al[95], Ivanov et al[96], Vdovin et al[97]). In these interesting experiments evidence of strong anomalous ion heating was found. For input powers of the order of 100 kW, pulse duration of less than one millisecond, the ion temperature was doubled from 50 to 100 eV. In addition, in some cases the plasma confinement was actually doubled due to the application of the rf power (Vdovin et al[97]). The anomalous ion heating was attributed to parametric decay into ion cyclotron waves and short wavelength drift waves, and the increased confinement time was attributed to stabilization of long wavelength drift waves. As shown in the above mentioned theoretical papers, additional instabilities may be expected to occur in multi-ion species plasmas.

4.7. Soliton Formation and Density Depletion.

In much of this paper we concentrated on parametric mode coupling effects and ignored the nonlinear modification of the

density. However, as discussed in the theoretical section, when the incident fields are sufficiently strong, the equilibrium density may be strongly modified by the ponderomotive force and the electric fields can be trapped in the density cavities. Such effects are particularly important in unmagnetized plasmas near the $\omega_o \simeq \omega_{pe}$ critical layer, where strong electric fields can build up (Freidberg et al[98]). These nonuniform localized electric fields then could produce energetic tails on the distribution function by accelerating particles to high energies (Freidbert et al[98], Bezzerides et al[99], Wong et al[100]). In addition, the modified density profiles could strongly alter the thresholds for parametric instabilities. Some of these effects have been observed in recent experiments by Kim et al[101] and Ikezi et al[102], and Wong and Stenzel[100]. In Fig. 22 we reproduced some of the results from the work of Ikezi et al[102] and Wong and Stenzel[100]. In particular, this figure shows that the density perturbations move away form the critical layer, and that trapped electric fields are localized in the density cavities. Furthermore, in the experiments of Ikezi et al it was observed that the coupled nonlinear electron-plasma wave and the nonlinear ion-acoustic wave propagate with approximately the ion acoustic velocity in the form of periodic wave trains. Nishikawa et al[103] developed a theory to deal with this special case. These processes may be of importance in situations where very strong rf fields are generated in the plasma.

5. SUMMARY AND CONCLUSIONS.

In the presence of sufficiently strong high frequency electric fields the plasma is subject to parametric instabilities. In this review we attempted to summarize the important developments in the theory of parametric instabilities, and gave a considerable

amount of experimental evidence for their existence. Although the first theoretical predictions of such instabilities in plasmas were given ten years ago, much of our present day understanding of this phenomena was obtained in the past five years. The explosive growth of this field has to do with possible applications to laser-pellet fusion and rf heating of magnetically confined fusion plasmas (and for a brief period ionospheric modification experiments). While there is now good theoretical and experimental understanding of linear theory in uniform or weakly inhomogeneous plasmas, our understanding of this phenomena in strongly inhomogeneous plasma is rather poor. Also, while there has been much progress in developing nonlinear theories, only in a narrow regime ($T_e = T_i$, $B = 0$, E_o close to threshold) are such theories capable of predicting the saturated state and the associated anomalous absorption. Even in this case, detailed experimental verification is either lacking or agreement between theory and experiment is not satisfactory. The distribution of absorbed energy between main body and/or a suprathermal tail is not well known. To present date most of the experimental information available has been obtained in small scale microwave experiments, or in computer simulations. Whether such experimental and/or theoretical results can be extrapolated to the highly complex geometries of laser pellet interaction and/or hot, magnetically confined fusion plasmas, remains to be seen. For example, in the case of laser pellet interaction in the few experimental results available the large energetic suprathermal electron tails predicted by computer simulations are not found. In addition, there is rather good absorption and not much reflection, in contrast to the predictions based on backscattering theories. In recent laser experiments it is found that

sharp gradients and strong (several mega-gauss) magnetic fields may be generated. Thus, the present theories may have to be modified significantly to take these effects into consideration.

In the case of magnetically confined plasmas to present date there have been only a few experiments in fusion (toroidal) plasmas. In these experiments the crucial questions are the heating efficiency and the effects of the excited turbulence upon plasma confinement. Clearly, if significant anomalous diffusion were produced rf heating would not be a satisfactory type of supplementary heating. Of course, these may depend on the particular frequency regime used to heat the plasma, and must be explored experimentally. For example, at the present time we expect such results to come in from a number of experiments in the regime of the lower hybrid frequency. This regime of frequencies is expected to be a favourable one for heating tokamaks.

In conclusion, we see that in the next few years important new experimental results will be available both in the field of laser fusion and from magnetically confined fusion plasmas which will test the importance of parametric theories, and which may generate further development of these theories. This will lead to a better basic understanding of collective and/or turbulent phenomena in plasmas.

*This work was supported by the Energy Research and Development Administration (formally U.S. Atomic Energy Commission) under contract E(11-1)-3073.

REFERENCES

1) DuBois, D. F., and Goldman, M. V., Phys. Rev. Lett. 14, (1965) 544; also Phys. Rev. 164,(1967) 207; Silin, V. P., Sov. Phys. JETP. 21, (1965) 1127; Jackson, E. A., Phys. Rev. 153, (1967) 203; Nishikawa, K., J. Phys. Soc. Japan 24, (1968) 916, 1152.

2) Kaw, P., and Dawson, J. M., Phys. Fluids 12, (1969) 2586.

3) Piliya, A. D., Zh. Tekh. Fiz. 36, (1966) 818 [Sov. Phys. Tech. Phys. 11, (1966) 609].

4) Galeev, A. A., Sagdeev, R. Z., Nuclear Fusion 13, (1973) 603.

5) Kruer, W. L., and Dawson, J. M., Phys. Fluids 15, (1972) 446.

6) Davidson, R. C., Methods in Nonlinear Plasmas Theory, (Academic Press, New York, 1972).

7) Aliev, Y. M., Silin, V. P., and Watson, C., Zh. Eksp. Teor. Fiz. 50, (1966) 943 [Sov. Phys. JETP 23, (1966) 626].

8) Amano, T., and Okamoto, M., J. Phys. Soc. Japan 26, (1969) 391.

9) Porkolab, M., Nuclear Fusion 12, (1972) 329; also in Symposium on Plasma Heating and Injection, Varenna, Italy, 1972 (Editrice Compositori, Bologna, Italy, 1973) p. 54.

10) Porkolab, M., Phys. Fluids 17, (1974) 1432.

11) Porkolab, M., in Symposium on Plasma Heating in Toroidal Devices, Varenna, Italy, 1974 (Editrice Compositori, Bologna, Italy, 1974) pp. 28-40.

12) Forslund, D. W., Kindel, J. M., and Lindmann, E. L., Phys. Rev. Lett. 29, (1972) 249.

13) Porkolab, M., Arunasalam, V., and Ellis, R. A., Jr., Phys. Rev. Lett. 29, (1972) 1438.

14) Forslund, D. W., Kindel, J. M., and Lindmann, E. L., Phys. Rev. Lett. 30, (1973) 739.

15) Eidman, K., and Sigel, R., in Laser Interaction and Related Plasma Phenomena, Vol. 3B (Plenum Press, New York, New York, 1974) p. 667.

16) DuBois, D. F., in Laser Interaction and Related Plasma Phenomena, Vol. 3A (Plenum Press, New York, New York 1974) p. 267.

17) Drake, J. F., Kaw, P. K., Lee, Y. C., Schmidt, G., Liu, C. S., and Rosenbluth, M. N., Phys. Fluids 17, (1974) 778.

18) Manheimer, W. M., and Ott, E., Phys. Fluids 17, (1974) 1413.

19) Louisell, W. H., Coupled Mode and Parametric Electronics (John Wiley and Sons, Inc., New York), 1960.

20) Silin, V. P., Zh. Eksp. Teor. Fiz. 51, (1966) 1842 [Sov. Phys. JETP 24, (1967) 1242].

21) Kroll, N. M., J. Appl. Phys. 36, (1965) 34; Bobroff, D. L., ibid, 36, (1965) 1760.

22) Porkolab, M., and Chang, R. P. H., Phys. Fluids 13, (1970) 2054.

23) Harker, K. J., and Crawford, F. W., J. Geophys. Res. 75, (1970 5459.

24) Perkins, F. W., and Flick, J., Phys. Fluids 14, (1971) 2012.

25) Rosenbluth, M. N., Phys. Rev. Lett.29, (1972) 565; also, Rosenbluth, M. N., White, R. B., Liu, C. S., Phys. Rev. Lett. 31, (1973) 1190.

26) Pesme, D., Laval, G., Pellat, R., Phys. Rev. Lett. 31, (1973) 203.

27) Liu, C. S., Rosenbluth, M. N., and White, R. B., Phys. Fluids 17, (1974) 1211.

28) DuBois, D. F., Forslund, D. W., and Williams, E. A., Phys. Rev. Lett. 33, 1013 (1974).

29) Forslund, D. W., Kindel, J. M., Lee, K., and Lindman, E. L., Phys. Rev. Lett. 34, (1975) 193. Also Phys. Rev. All, (1975)679.

30) Nicholson, D. W., and Kaufman, A. N., Phys. Rev. Lett. 33, (1974) 1207.

31) Spatchek, K. H., Shukla, P. K.,and Yu, M. Y., Phys. Lett. 51A, (1975) 183.

32) Valeo, E., and Oberman, C., Phys. Rev. Lett. 30, (1973) 1035.

33) Thomson, J. J., Nuclear Fusion 15, (1975) 237.

34) Pustovalov, V. V., and Silin, V. P., Zh. Eksp. Teor. Fiz. 59, (1970) 2215 [Sov. Phys. JETP. 32, (1971) 1198].

35) DuBois, D. F., and Goldman, M. V., Phys. Fluids 15, (1972) 919.

36) Valeo, E., Oberman, C., and Perkins, F. W., Phys. Rev. Lett. 28, (1972) 340.

37) Fejer, J. A., and Kuo, Y. Y., Phys. Rev. Letts. 29, (1972) 1667.

38) DuBois, D. F., Goldman, M. V., and McKinnis, D., Phys. Fluids 16, (1974) 2257.

39) Bezzerides, B., and Weinstock, J., Phys. Rev. Letts 28, (1972) 481. Weinstock, J., and Bezzerides, B., Phys. Fluids 16, (1973) 2287; also Phys. Rev. Lett. 32, (1974) 754.

40) Kruer, W. L., Dawson, J. M., Phys. Fluids 15, (1972) 446.

41) DeGroot, J., Katz, J., Phys. Fluids 16, (1973) 401; also Bodner, S. E., Chapline, G. F., and DeGroot, J., J. Plasma Physics 15, (1973) 21.

42) Thomson, J. J., Faehl, R. J., Kruer, W. L., and Bodner, S. E., Phys. Fluids 17, (1974) 973.

43) Zakharov, V. E., Zh. Eksp. Teor. Fiz. 62, (1972) 1475 [Sov. Phys. JETP 35, (1972) 908]; also, Zakharov, V. E., and Kuznetsov, E. A., Zh. Eksp. Teor. Fiz. 66, (1974) 594 [Sov. Phys. JETP 39, (1974) 285].

44) Karpman, ., Plasma Physics, 13, (1971) 477.

45) Morales, G. J., Lee, Y. C., and White, R. B., Phys. Rev. Lett. 32, (1974) 457; also, Morales, G. J., and Lee, Y. C., Phys. Rev. Lett. 33, (1974) 1016.

46) Valeo, E. J., and Kruer, W. L., Phys. Rev. Lett. 33, (1974) 750; also Valeo, E. J., and Estbrook, K. G., Phys. Rev. Lett. 34, (1975) 1008.

47) Kaufman, A. N., and Stenflo, L., Bull. Am. Phys. Soc. 19, (1974) 938.

48) Hasegawa, A., Plasma Instabilities and Nonlinear Effects (Springer Verlong, Berlin, New York, 1975) p. 194.

49) Schmidt, G., Phys. Rev. Lett. 34, (1975) 724.

50) Stern, R. A., and Tzoar, N., Phys. Rev. Lett. 17, (1966) 903; also, Hiroe, S., and Ikegami, H., Phys. Rev. Lett. 19, (1967) 1414.

51) Chang, R. P. H., and Porkolab, M., Phys. Fluids 13, (1970) 2766; also, Phys. Rev. Lett. 25, (1970) 1262; also, Phys. Fluids 15, (1972) 297.

52) Chang, R. P. H., Porkolab, M., and Grek, B., Phys. Rev. Lett. 29, (1972) 206.

53) Stenzel, R., and Wong, A. Y., Phys. Rev. Lett. 28, (1972) 274.

54) Franklin, R. N., Hamberger, S. M., Lampis, G., and Smith, G. J., Phys. Rev. Lett. 27, (1971) 1119.

55) Gekker, I. R., and Sizukhin, O. V., Zh. Pis. Red. 9, (1969) 408. [Sov. Phys. JETP. Lett. 9, (1969) 243]; also, Proc. 9th Int. Conf. on Phenomena in Ionized Gases, Bucharest, 1969 p. 542.

56) Batanov, G. M., and Sarksyan, K. A., Zh. Pis. Red. 13, (1971) 539 [Sov. Phys. JETP Lett. 13, (1971) 384); also, Batanov, G. M., Sarksyan, K. A., and Silin, V. A., Proc. 9th Int. Conf. on Phenomena in Ionized Gases, Bucharest, 1969, p. 541; also

Sergeichev, K. F., and Trofimov, V. E., Zh. Pis. Red. 13, (1971) 236 [Sov. Phys. JETP Lett. 13, (1971) 166]; also, Proc. 9th Int. Conf. on Phenomena in Ionized Gases, Bucharest (1969) p. 540.

57) Eubank, H., Phys. Fluids 14, (1971) 2551.

58) Dreicer, H., Ingraham, C., and Henderson, D., Phys. Rev. Lett. 26, (1971) 1616; also, Fifth European Conference on Controlled Fusion and Plasma Physics, Grenoble, France, (1972).

59) Chu, T. K., and Hendel, H., Phys. Rev. Lett. 29, (1972) 634.

60) Flick, J., Ph. D. Thesis, Department of Astrophysical Sciences, Princeton University (1975).

61) Demirkhanov, R. A., Khorasanov, G. L., and Sidorova, I. K., Zh. Eksp. Teor. Fiz. 59, (1970) 1873 [Sov. Phys. JETP 32, (1971) 1013].

62) Vdovin, V. L., et al. Zh. Pis. Red. 14, (1971) 228 [Sov. Phys. JETP Lett. 14, (1971) 149].

63) Utlaut, W. F., and Cohen, Science 174, (1971) 245.

64) Wong, A. Y., and Taylor, R. J., Phys. Rev. Lett. 27, (1971) 644.

65) Carlson, H. C., Gordon, W., and Showen, R. L., J. Geophys. Res. 77, (1972) 1242.

66) Grek, B., and Porkolab, M., Phys. Rev. Lett. 30, (1973) 836; also, to be published; also, Grek, B., Ph. D. Thesis, Department of Astrophysical Sciences, Princeton University, Princeton, N. J., (1975).

67) Porkolab, M., Arunasalam, V., Luhmann, N. C., Jr., and Schmitt, J. P. M., Princeton Plasma Physics Laboratory Report MATT-1160 (1975)(to be published).

68) Okabayashi, M., Chen, K., and Porkolab, M., Phys. Rev. Lett. 31, (1973) 1113.

69) Dreicer, H., Ellis, R. F., and Ingraham, J. C., Phys. Rev. Lett. 31, (1973) 426.

70) Mizuno, K., and Degroot, J. S., Phys. Rev. Lett. 35, (1975) 219.

71) Porkolab, M., Arunasalam, V., and Luhmann, N. C., Jr., Electromagnetic Wave Propagation Panel Symposium, Edinburgh, Scotland, 1973 (Technical Editing and Reproduction Ltd., Harford House, London, p. D8 (1974)); also, Plasma Physics 17, (1975) 405.

72) Hendel, H. W., and Flick, J. T., Phys. Rev. Lett. 31, (1973) 199.

73) Chu, T. K., Bernabei, S., and Motley, R. W., Phys. Rev. Lett. 31, (1973) 211.

74) Bernabei, S., Chu, T. K., Hooke, W. M., and Motley, R. W., Bull. Am. Phys. Soc. 18, (1973) 1314; also, 2nd Topical Conference on R.F. Plasma Heating, Texas Tech University, Lubbock, Texas (1974) pp. C5. Motley, R. W., Bernabei, S., Hooke, W. M., and Jassby, D. L., Princeton Plasma Physics Laboratory Report 1117 (1975).

75) Edgley, P. D., Franklin, R. N., Hamberger, S. M., and Motley, R. W., Phys. Rev. Lett. 34, (1975) 1269.

76) Trivelpiece, A. W., Gould, R. W., J. Appl. Phys. 30, (1959) 1784.

77) Farenik, V. I., Vlasov, V. V., Rozhkov, A. M., Zh. Pis. Red. 18, (1973) 409 [Sov. Phys. JETP Lett. 18 (1973) 240].

78) Chang, R. P. H., and Porkolab, M., Phys. Rev. Lett. 31, (1974) 1227; also, ibid, 31, (1973) 1241.

79) Brusati, M., Cima, G., Fontanesi, M., and Sindoni, E., Lettere al Nuovo Cimento, 10, (1974) 67.

80) Porkolab, M., Princeton Plasma Physics Laboratory Report MATT-1069 (1974).

81) Kindel, J. M., Okuda, H., and Dawson, J. M., Phys. Rev. Lett. 29, (1972) 995.

82) Berger, R. L., and Perkins, F. W., Princeton Plasma Physics Laboratory Report MATT-1130 (1975).

83) Karney, C. F. F., Bers, A., and Kulp, J. L., Bull. Am. Phys. Soc. 18, (1973) 1273.

84) Rogister, A., Phys. Rev. Lett. 34, (1975) 80.

85) Ott, E., Phys. Fluids 18, (1975) 566.

86) Glagolev, V. M., Krivov, N. A., Skosyrev and Yu, V., in Proceedings of the Fourth International Conference on Plasma Physics and Controlled Nuclear Fusion Research (International Atomic Energy Agency, Vienna, 1971) Vol. II,

87) Grigoreva, L. I., Sizenko, V. L., Smerdov, B. I., Stepanov, K. N., and Chechkin, V. V., Zh. Eksp. Teor. Fiz. 60, (1971) 605 [Sov. Phys. JETP 33, (1971) 329].

88) Kitsenko, A. B., Panchenko, V. I., Stepanov, K. N., Tarasenko, V. F., Nuclear Fusion 13, (1973) 557.

89) Sundaram, A. K., and Kaw, P. K., Nuclear Fusion 13, (1973) 901.

90) Ivanov, A. A., and Parail, V. V., Zh. Eksp. Teor. Fiz. 62, (1972) 932 [Sov. Phys. JETP 35, (1972) 494].

91) Sperling, J. L., and Perkins, F. W., Phys. Fluids 17, (1974) 1857.

92) Kitsenko, A. B., and Stepanov, K. N., Zh. Eksp. Teor. Fiz. 64, (1973) 1606 [Sov. Phys. JETP 37, (1973) 813]; also, Kitsenko, A. B., Panchenko, V. I., and Stepanov, K. N., Zh. Tekh. Fiz. 43, (1973) 1422, 1426, 1437 [Sov. Phys. Tech. Phys. 18, (1974) 902, 905, 911].

93) Harms, K. D., Hasselberg, G., Rogister, A., Nuclear Fusion 14, 251 (1974); ibid 14, 657 (1974).

94) Martinov, N., Samain, A., Plasma Physics 15, (1974) 783.

95) Voloskko, A. Y., Voitsenya, V. S., Lanyinov, A. V., Miroshnichenko, G. A., Nizhnik, G. Y., and Solodovchenko, S. I., Zh. Pis. Red. 16, (1972) 80 [JETP Letts. 16, (1972) 54]; also, Voitsenya, V. S., Voloshko, A. Y., Longinov, A. V., Miroshnickhenko, G. A., Nizhnik, G. Y., Solodovchenko, S. I., Proc. Fifth European Conf. Controlled Fusion and Plasma Physics, Grenoble 1, (1972) 111.

96) Ivanov, N. V., Kovan, I. A., Koslov, L. I., Los', E. V., Svishchev, V. S., Shvindt, N. N., Zh. Pis. Red. 16, (1972) 88 [Sov. Phys. JETP Lett. 16, (1972) 60].

97) Vdovin, V. L., Zinov'ev, O. A., Ivanov, A. A., Kozorovitskii, L. L., Parail, V. V., Rakhimbabaev, Ya. R., Rusanov, V. D., Zh. Pis. Red. 14, (1971) 228; [Sov. Phys. JETP Lett. 14, (1971) 149]; also, Zh. Pis. Red. 17, (1973) 4 [Sov. Phys. JETP Lett. 17, (1973) 2].

98) Freidberg, J. P., Mitchell, R. W., Morse, R. L., and Rudsinski, L. J., Phys. Rev. Lett. 28, (1972) 795.

99) Bezzerides, B., and DuBois, D. F., Phys. Rev. Lett. 34, (1975) 1381.

100) Wong, A. Y., and Stenzel, R. L., Phys. Rev. Lett. 34, (1975) 727.

101) Kim, H. C., Stenzel, R. L., and Wong, A. Y., Phys. Rev. Lett. 33, (1974) 886.

102) Ikezi, H., Nishikawa, K., and Mima, K., Phys. Soc. Japan 37, (1974) 766; also, Proceedings Fifth International Conference on Plasma Physics and Controlled Nuclear Fusion Research, Tokyo, (1974).

103) Nishikawa, K., Hojo, H., and Mima, K., Phys. Rev. Lett. 33, (1974) 148.

TABLE 1. TYPICAL THRESHOLDS IN MAGNETIZED PLASMA

PUMP WAVE	DECAY WAVE	THRESHOLD
Extraordinary Mode (if ignore tunneling) $(E_\perp B_o)$; $\omega_o \simeq \omega_{UH}$ $(\omega_{pe} << \Omega_e)$	Lower-Hybrid Upper-Hybrid	$\frac{\omega_{pe}}{\sqrt{2\Omega_e\omega_1}}\sqrt{\frac{\gamma_1\gamma_2}{\omega_1\omega_2}} \lesssim \frac{E_o}{8\sqrt{\pi n_o T_e}}$
Extraordinary Mode (if ignore tunneling) $(E_\perp B_o)$; $\omega_o \simeq \omega_{UH}$ $(\omega_{pe} << \Omega_e)$	Ion Acoustic Upper-Hybrid	$\frac{\omega_2}{\omega_{pe}}\sqrt{\frac{\gamma_1\gamma_2}{\omega_1\omega_2}} \lesssim \frac{E_o}{8\sqrt{\pi n_o T_e}}$
Ordinary Mode $(\omega_o \gtrsim \omega_{pe})$	Ion Acoustic Electron Plasma	$\sqrt{\frac{\gamma_1\gamma_2}{\omega_1\omega_2}} \lesssim \frac{E_o}{8\sqrt{\pi n_o T_e}}$
Electron Plasma Wave (Trivelpiece-Gould)	Ion Acoustic (Ion Cyclotron) Electron Plasma	$\frac{\omega_o\Omega_e}{\omega_{pe}^2}\sqrt{\frac{\gamma_1\gamma_2}{\omega_1\omega_2}(1+\frac{\omega_{pe}^2}{\Omega_e^2})} \lesssim \frac{E_o}{8\sqrt{\pi n_o T_e}}$
Whistler Wave $\omega_o < \Omega_e < \omega_{pe}$	Ion Acoustic Electron Plasma	$\frac{\omega_o(\Omega_e-\omega_o)}{\omega_{pe}^2}\sqrt{\frac{2\gamma_1\gamma_2}{\omega_1\omega_2}(1+\frac{\sin^2\theta\omega_{pe}^2\Omega_e^2}{(\omega_2^2-\Omega_e^2)^2}} \lesssim \frac{E_o}{8\sqrt{\pi n_o T_e}}$
Lower-Hybrid Wave (Resonance Cone, Whistler Wave) $k_\parallel/k \lesssim 3\sqrt{m_e/m_i}$	Lower-Hybrid Ion Quasi-Mode	$\frac{\Omega_e\omega_o}{2\omega_{pe}^2}\left(\frac{2.6\gamma_2}{\omega_2}(1+\frac{\omega_{pe}^2}{\Omega_e^2}\right)^{1/2} \lesssim \frac{E_o}{8\sqrt{\pi n_o T_e}}$
	Lower-Hybrid Purely Growing Mode	$\frac{\Omega_e\omega_o}{2\omega_{pe}^2}\left(\frac{2\gamma_2}{\omega_2}(1+\frac{\omega_{pe}^2}{\Omega_e^2}\right)^{1/2} \lesssim \frac{E_o}{8\sqrt{\pi n_o T_e}}$
Magnetosonic Wave $(\omega_o \simeq \Omega_i)$	Ion Cyclotron Drift Wave	$2\sqrt{\omega^*\Omega_i} \lesssim \frac{kcE_o}{B}$

TABLE 2. SUMMARY OF EARLY EXPERIMENTS

GEOMETRY	GROUP	POL.	THRESH.	SPECTR.	PUMP	DECAY WAVES	ANOM.ABS.	HEATING
WAVEGUIDE	Gekker Sizukhin	B = 0	(?)	NO	$\omega_o \simeq \omega_{pe}$	NO	YES	NO
	Batanov Sergeichev	E ⊥ B	NO	NO	$\omega_o \gtrsim \Omega_e$	NO	NO	YES
	Eubank	E ∥ B E ⊥ B	(?)	LOW F. YES	$\omega_o \gtrsim \omega_{pe}$ $\omega_o \gtrsim \Omega_e$	NO	YES	YES
CAVITY	Dreicer Ingraham	E ∥ B	YES	(?)	$\omega_o \gtrsim \omega_{pe}$	NO	YES	YES
	Chu Hendel	E ∥ B	YES	YES	$\omega_o \gtrsim \omega_{pe}$	NO	YES	YES
GRID	Stenzel Wong	B = 0	YES	YES	$\omega_o \simeq \omega_{pe}$	YES	NO	NO
	Chang Porkolab	E ⊥ B	YES	YES	$\omega_o \gtrsim \Omega_e$	YES	NO	NO
	Franklin et al	E ∦ B	YES	YES	$\omega_o < \omega_{pe}$	YES	NO	NO
SLOW-WAVE ST.	Porkolab Arunasalam	E ∦ B	YES	YES	$\omega_o \gtrsim \Omega_e$	YES	YES	YES
DISCHARGE T. IN WAVEGUIDE	Stern Tzoar	B = 0	NO	YES	$\omega_o \simeq \omega_{pe}$	?	NO	NO
	Hiroe Ikegami	E ⊥ B	NO	YES	$\omega_c \simeq \omega_{UH}$	?	NO	NO
TOKAMAK	Vdovin, et al.	-	-	?	MAGNETOSONIC WAVE		YES	NO

TABLE 3. SUMMARY OF EXPERIMENTS

PUMP WAVES	DECAY WAVES	GEOMETRY	HEATING	AUTHORS
Extraordinary Mode ($\omega_o \simeq \omega_{UH}, n\Omega_e$)	Bernstein Lower Hybrid Ion Acoustic	Grids (Linear discharge)	T_e (main body, tail)	Grek, Porkolab
		3 cm microwave (RF discharge)	T_e (main body, tail)	Porkolab et al
		3 cm microwave (Toroidal Spherator) (FM-1)	T_e (main body) T_i (main body)	Okabayashi, et al
Electron Plasma Wave (O mode, or Trivelpiece-Gould, or B = 0) ($\omega_{pi} << \omega_o \lesssim \omega_{pe}$)	Electron Plasma Ion Acoustic	Microwave Horn Slow-wave structure (Linear RF discharge)	T_e (tail, main body) T_e (tail), T_i (tail)	Porkolab et al
		Plasma in Waveguide (B = O)	T_e (tail)	Mizuno, Degroot
	Electron Plasma Ion Acoustic	Cavity (Q-machine)	T_e (main body) T_i (main body)	Hendel, Flick
	Electron Plasma Ion Cyclotron	Capacitor Plates (Q-machine)	T_i (main body) T_e (?)	Chu, et al
	Electron Plasma Ion Acoustic	Capacitor Plates or Split Cylinders (RF discharge)	T_i (main body)	Bernabei, et al Tolnas, et al Motley, et al

TABLE 4. SUMMARY OF EXPERIMENTS

PUMP WAVE	DECAY WAVES	GEOMETRY	HEATING	AUTHORS
Lower-Hybrid Slow Wave $\omega_{pi} \lesssim \omega_o$	Lower Hybrid Ion Acoustic Ion Cyclotron	Semi-cylinders (Linear discharge)	T_i (energetic ions)	Farenik et al
		Slow-Wave Structure	T_e (main body)	Brusati et al
Coaxial Mode (Lower-Hybrid) ($\omega_{pi} \lesssim \omega_o$)	Lower-Hybrid Ion-Quasi Mode Purely Growing Mode	Capacitor Plates Coaxial Capacitor (Linear discharge)	T_e, T_i (main body, tail)	Chang, Porkolab
Whistler $\omega_o \lesssim \omega_{ce} < \omega_{pe}$	Whistler Electron Plasma Ion Acoustic Ion-Quasi Mode	Slow-Wave Structure (Linear RF discharge)	T_e, T_i (tail)	Porkolab, et al
Whistler or Magnetosonic $\omega_o \lesssim \omega_{pi}$	Lower-Hybrid Ion Acoustic Modified Two-Stream	Helix (Linear discharge)	T_e, T_i (main body, tail)	Grigoreva et al Kitsenko et al Glagolev et al
Slow Wave $\omega_{ci} \lesssim \omega_o < \omega_{LH}$	Ion Acoustic Ion Cyclotron Lower Hybrid	Surface electrodes (Stellarator-Torsatron)	T_e, T_i (main body)	Voloshiko et al Voitsenya et al
Magnetosonic $\omega_{ci} \simeq \omega_o$	Ion Cyclotron Drift Wave	Loop (Tokamak)	T_i (main body)	Ivanov et al Volovin et al

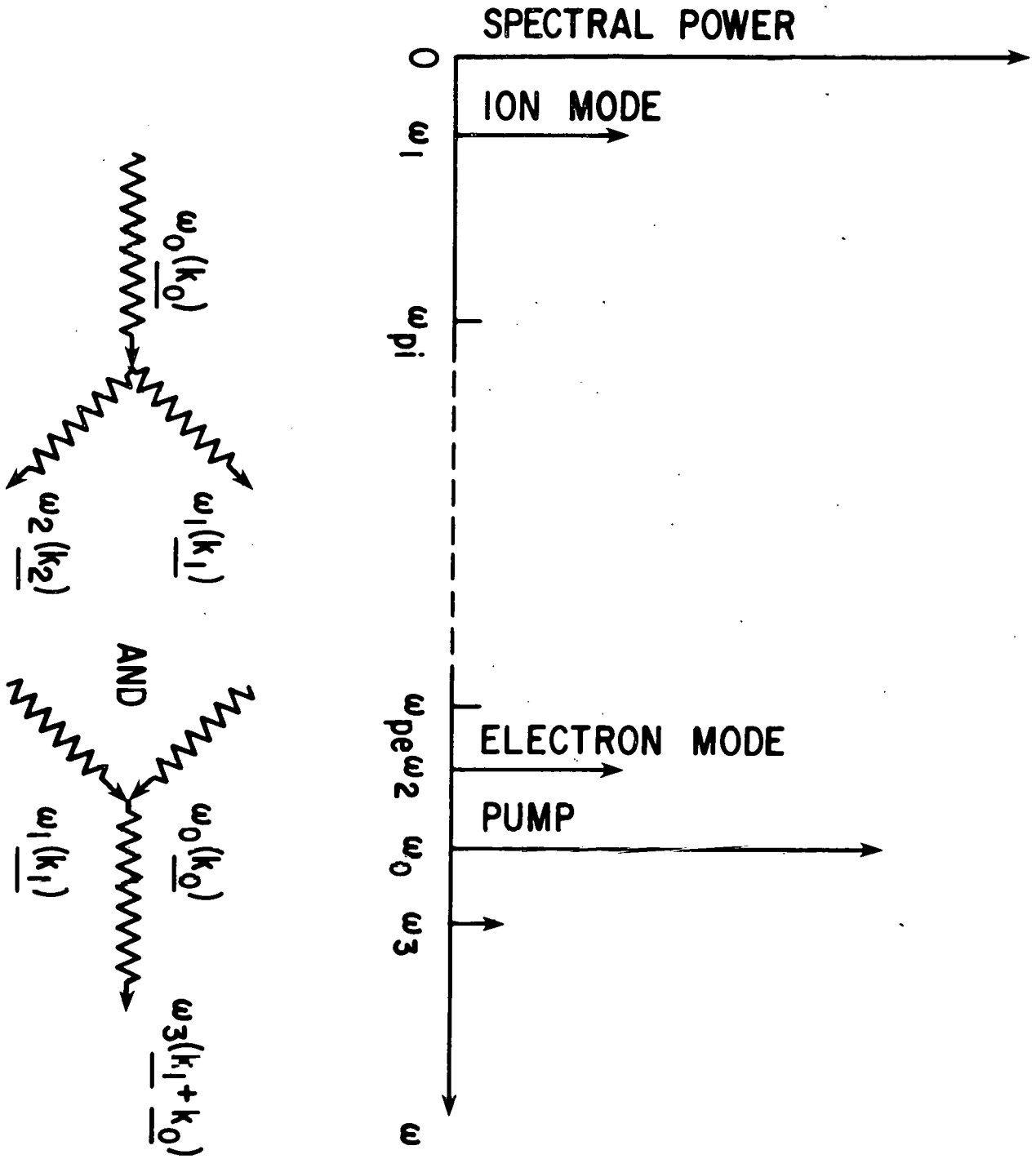

Fig. 1. Typical frequency spectrum for the parametric decay instability. Also shown are the corresponding scattering diagrams.

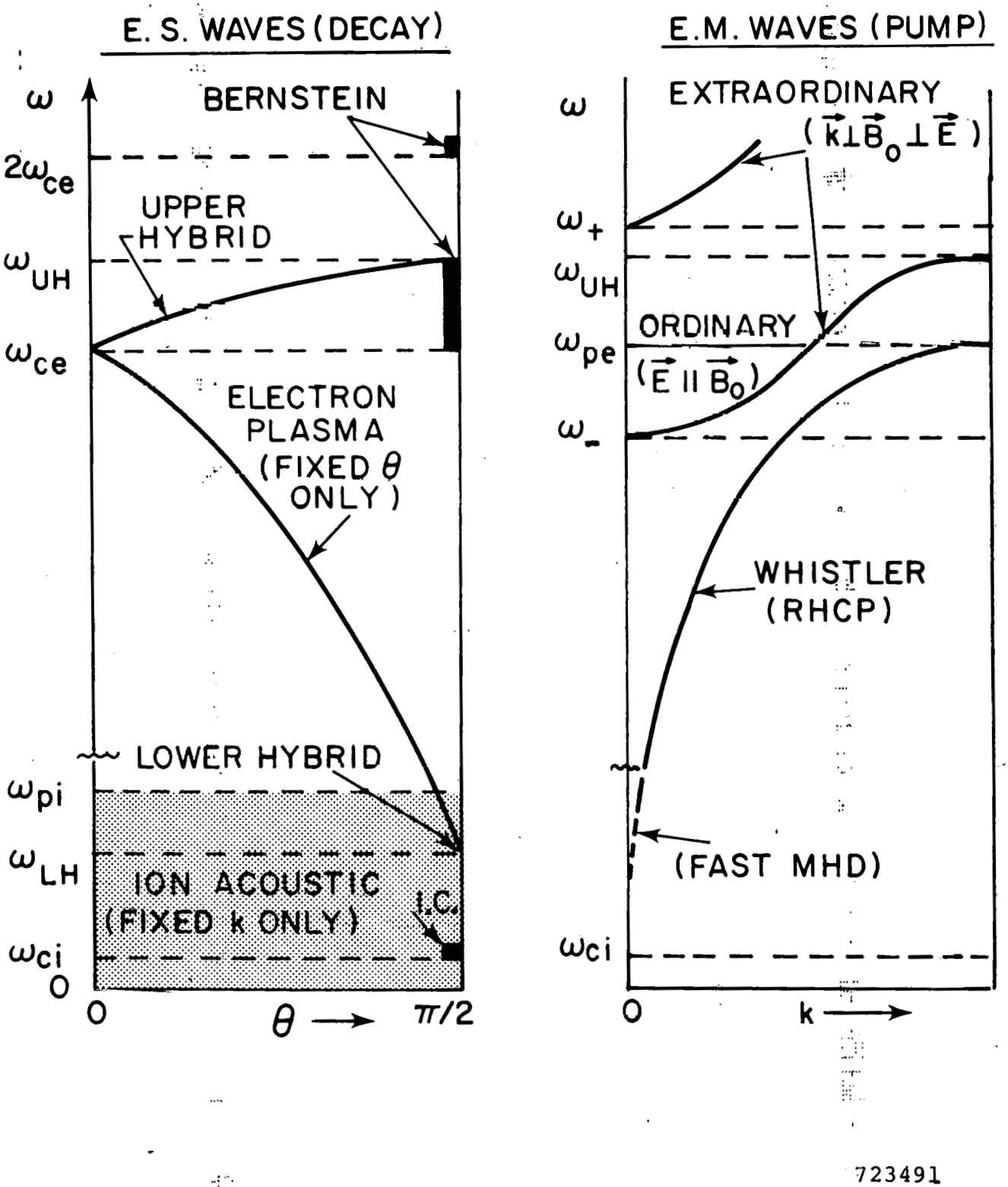

723491

Fig. 2. A schematic of possible choices for pump waves and decay waves in a magnetized plasma. θ designates the angle of propagation with the magnetic field.

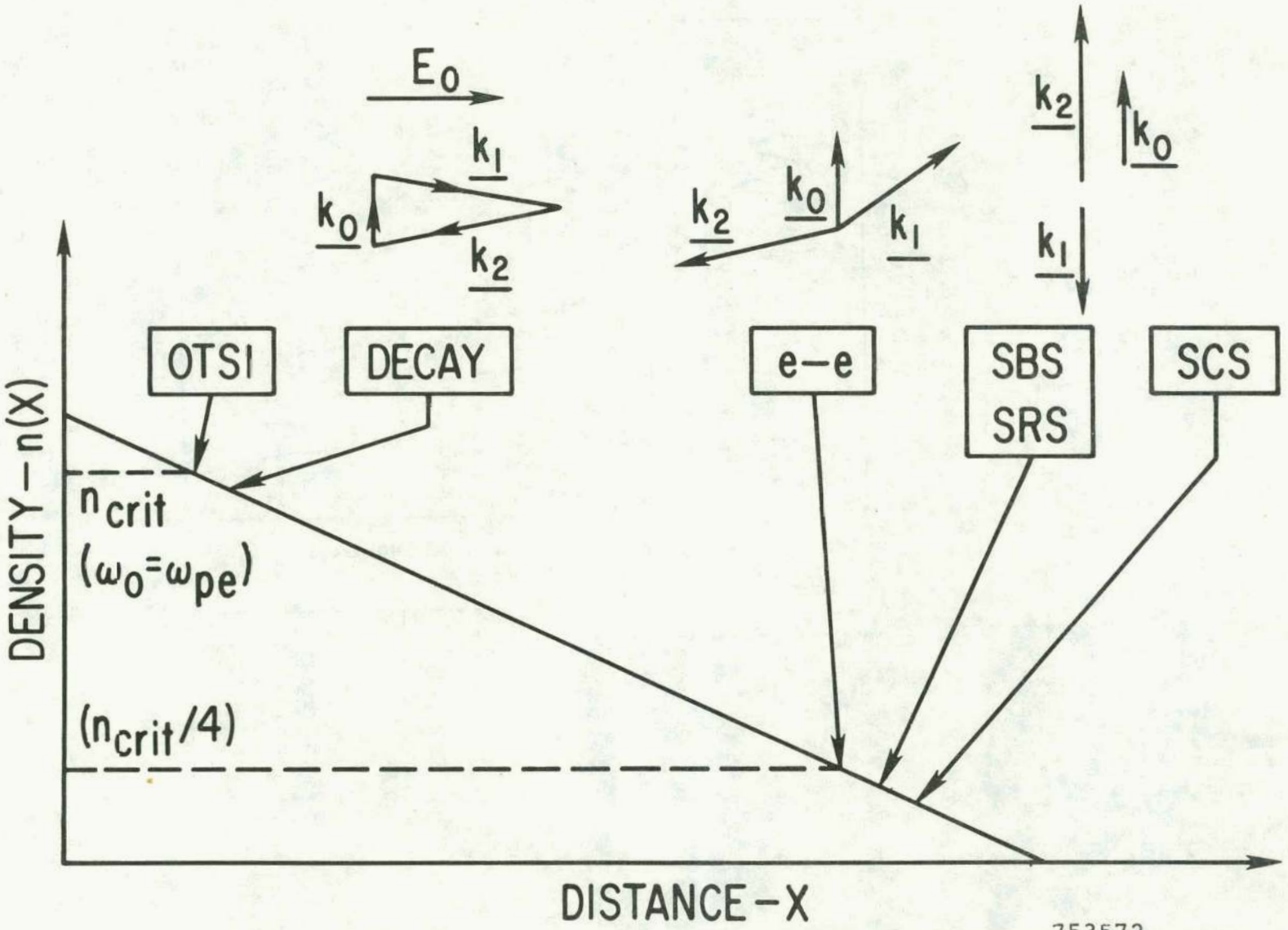

Fig. 3. "Theoretician's model" of inhomogeneous plasma with linearly varying density gradient. Also shown are locations of instabilities of possible importance in laser fusion schemes, including some momentum diagrams. OTSI designates the purely growing mode, (EE)designates the $\omega_o \simeq 2\omega_{pe}$ instability, and (SBS),(SRS), and (SCS) designate stimulated Brillouin, Raman, and Compton scatter, respectively.

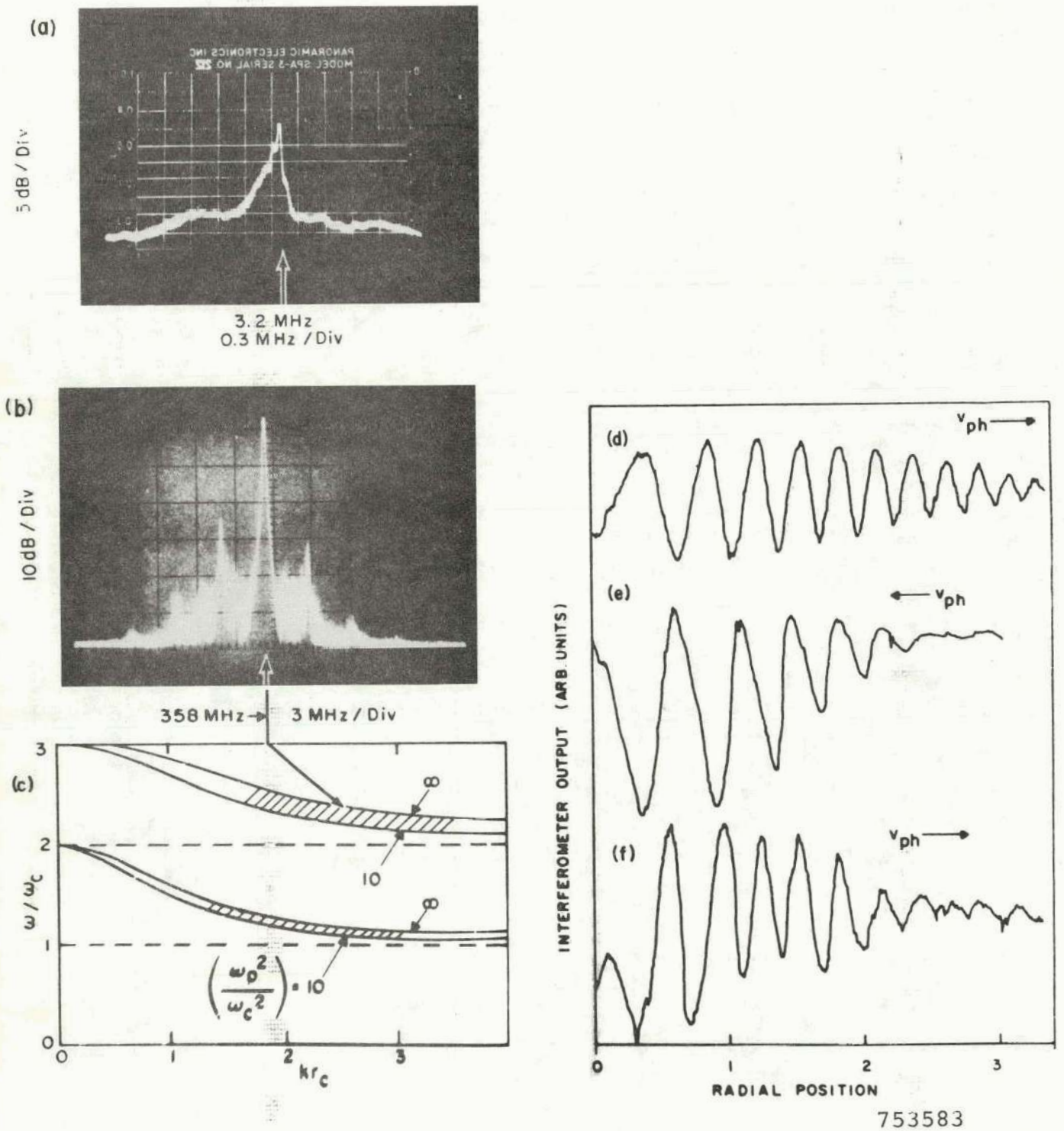

Fig. 4. Decay spectrum showing energy (frequency) conservation of: (a) low frequency ion acoustic waves, (b) high frequency cyclotron harmonic (Bernstein) waves, when pumped by $E_o \perp B$ in the shaded regions of the dispersion curves of cyclotron harmonic waves; (c) the momentum conservation is verified from the interferometer traces of the waves; (d) ion acoustic wave, (e) lower sideband (Bernstein wave) (f) upper sideband (Bernstein wave) (After Chang, Porkolab and Grek[52]).

I.R. Gekker and O. V. Sizukhin, 1969;

$B = 0$

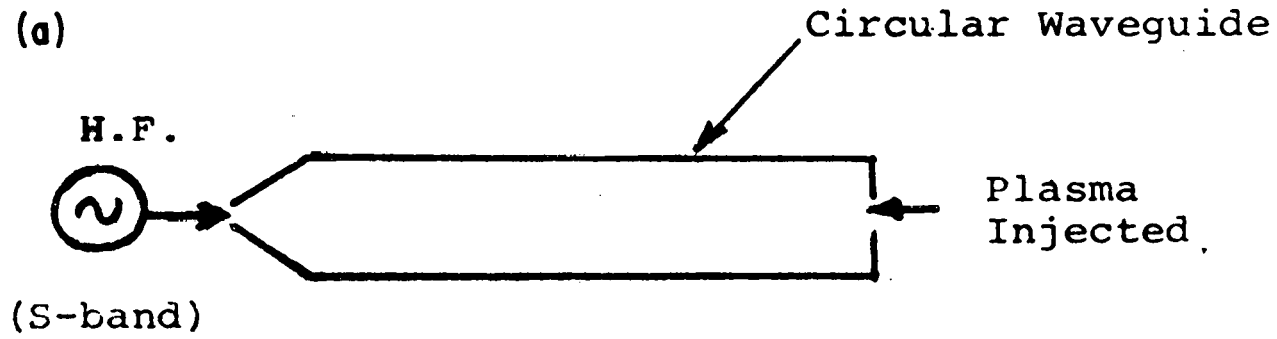

$$\nu_{ei} < \omega < \omega_P$$

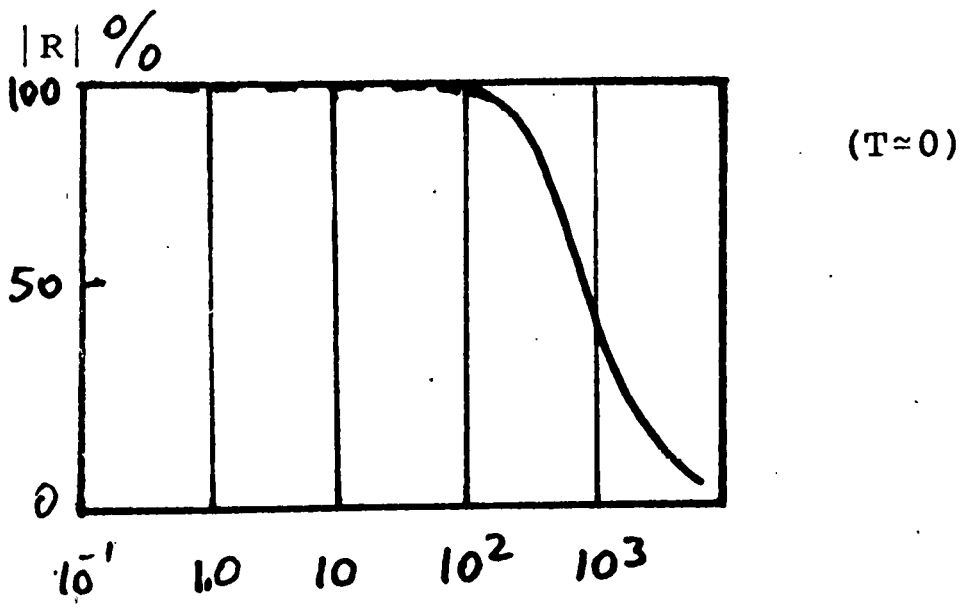

For 100V/cm, $V_E/V_{th} = \frac{eE}{m\omega} \Big/ V_{th} \simeq 0.1$

753581

Fig. 5(a) Experimental setup of Gekker and Sizukhin[55]

(b)

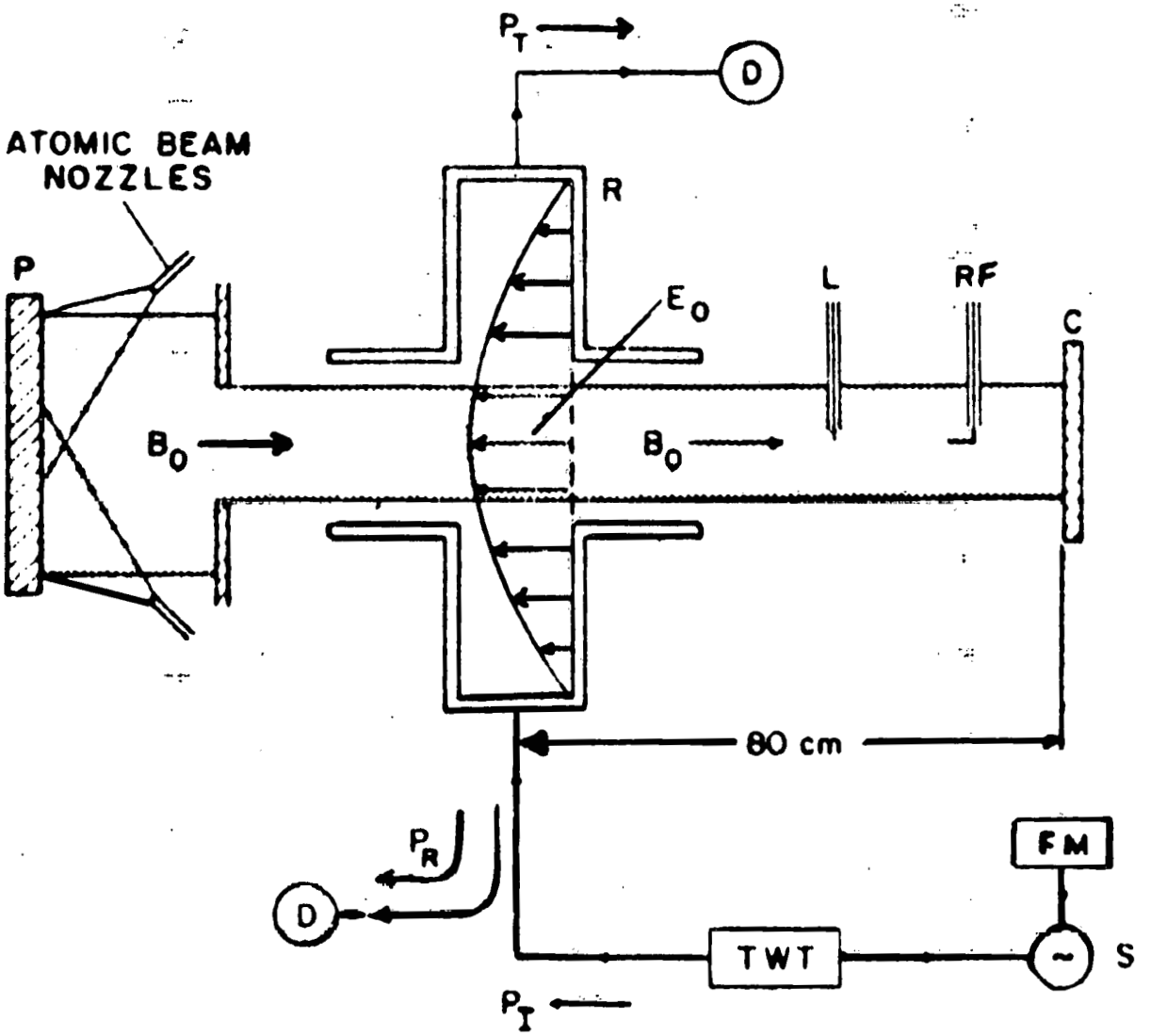

753582

Fig. 5(b) Typical arrangement of cavity measurements of anomalous absorption (after Dreicer et al.[58])

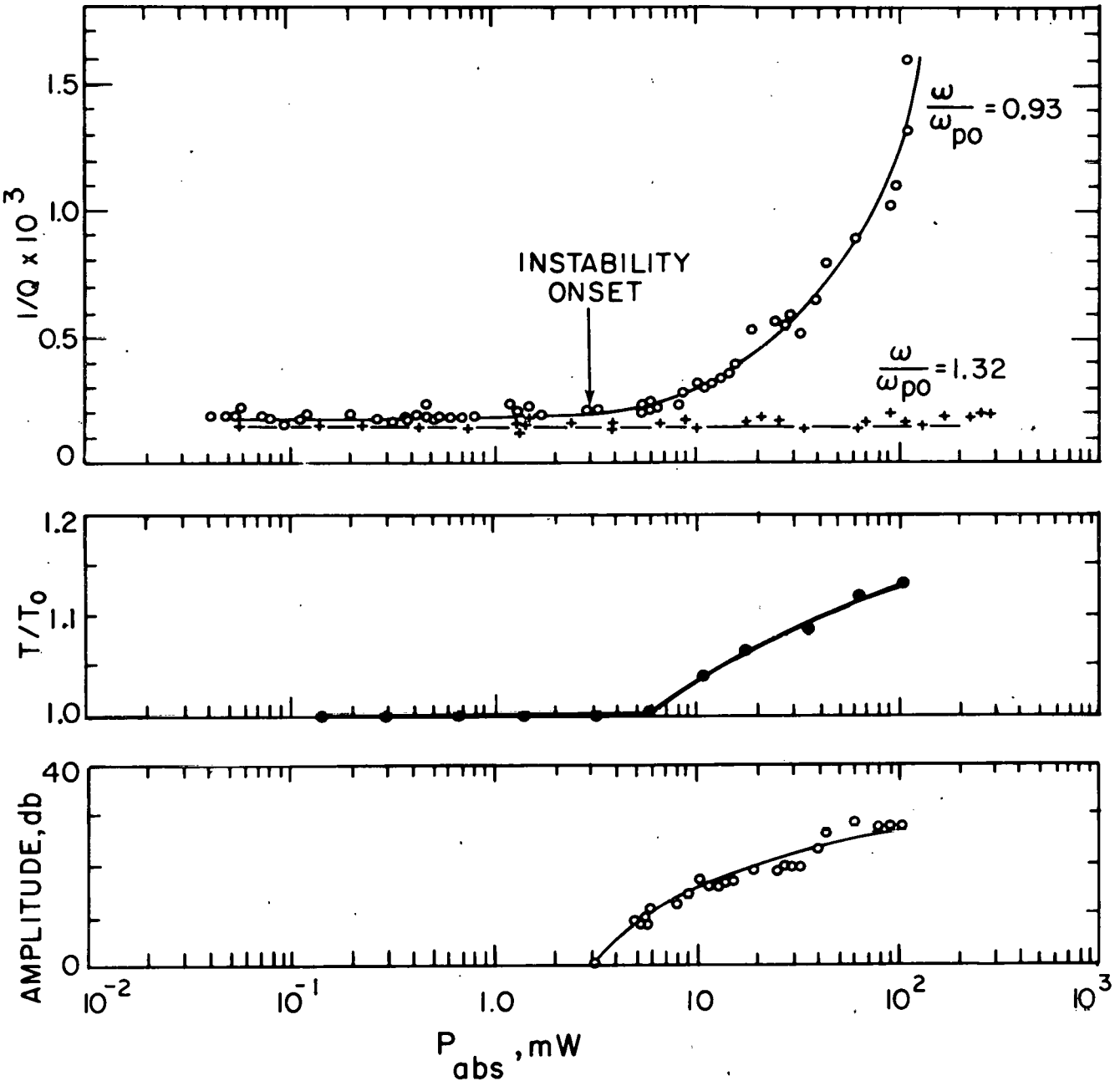

723160

Fig. 6. Measurements of the cavity Q, temperature, and fluctuation amplitude in the experiments of Chu and Hendel[59].

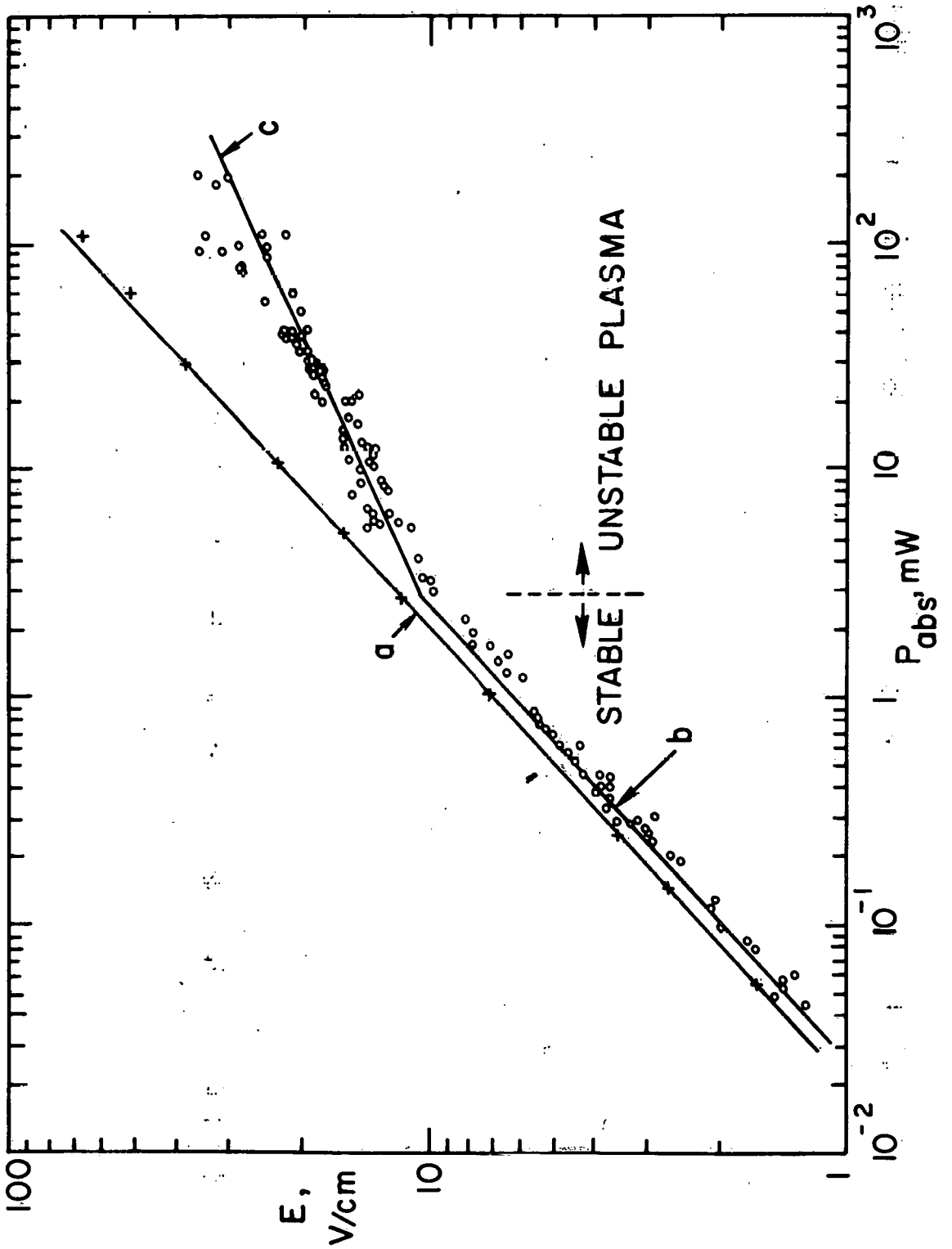

723180

Fig. 7. Results of the power absorption measurements in the experiments of Chu and Hendel[59].

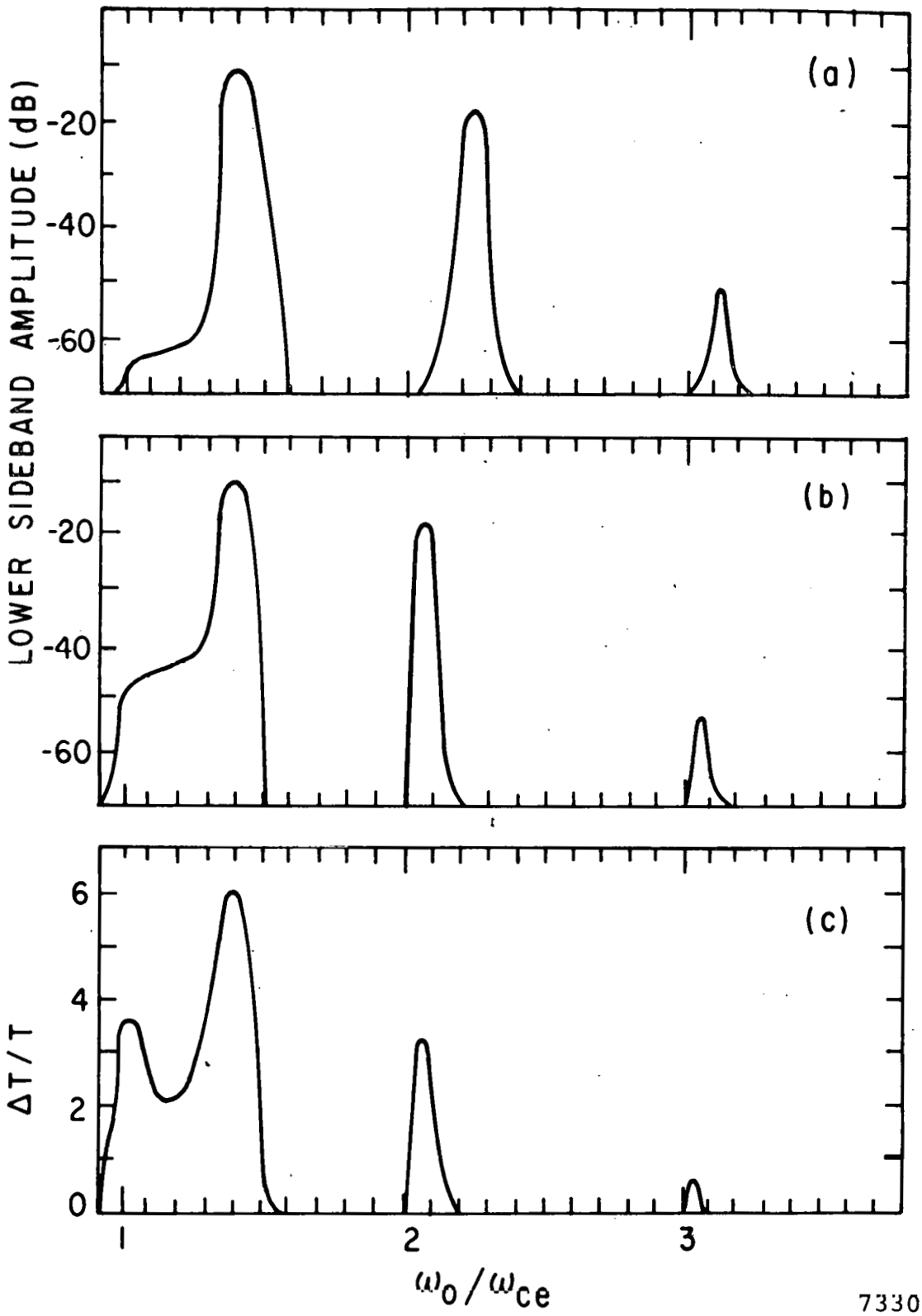

Fig. 8. (a) Amplitudes of Bernstein waves which couple with lower hybrid waves; $\omega_{ce} = \omega_{pe}$; ω_o (the pump frequency) is varied. (b) Amplitudes of Bernstein waves which couple with ion-acoustic waves. (c) Fractional increase of the main electron body temperature as obtained from a swept Langmuir probe; $P_o \simeq 30$ W. (After Grek and Porkolab[66]).

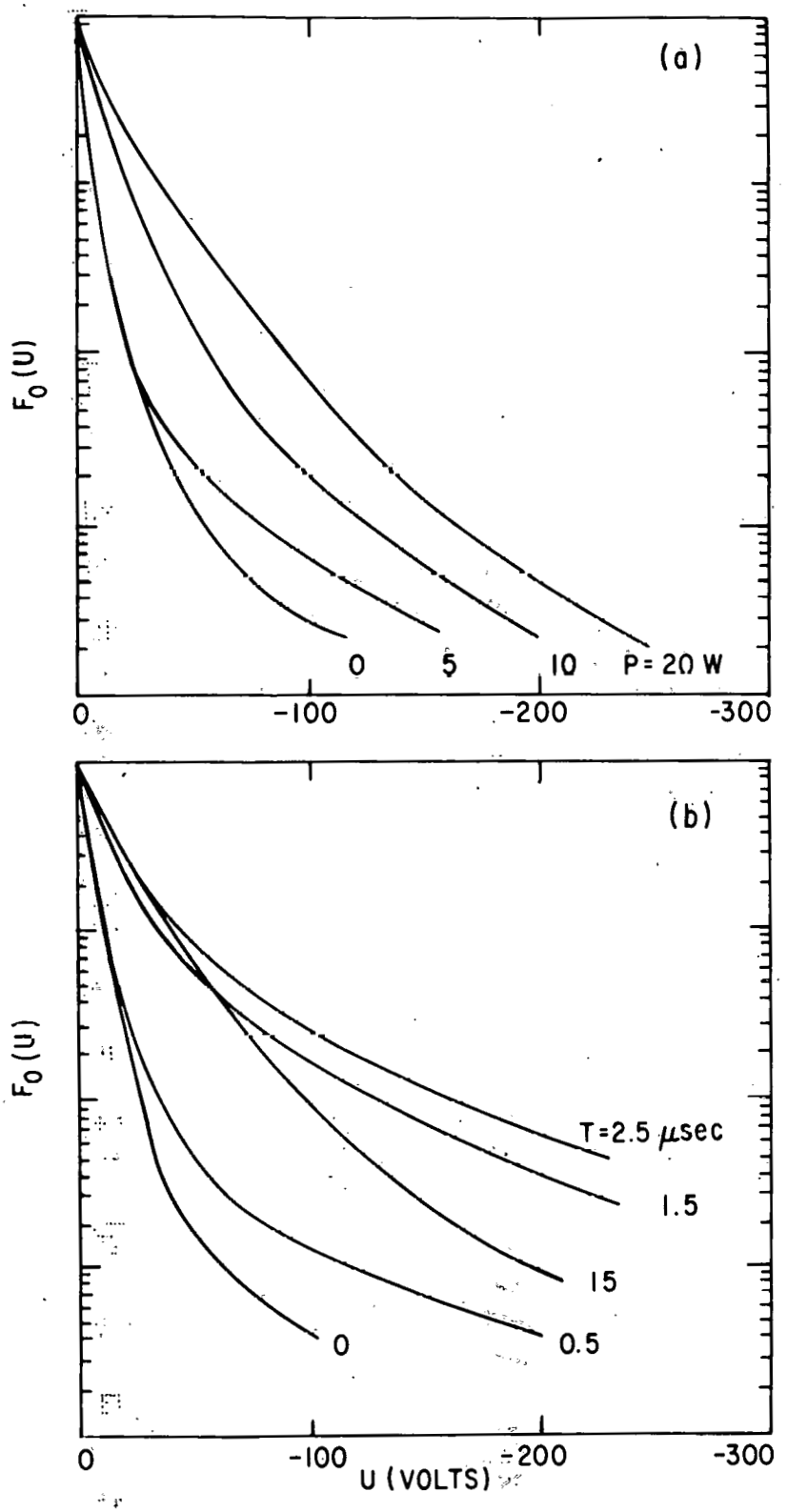

733046

Fig. 9. (a) Electron energy distribution [$F_o(\mu)$] for different powers (P) 5 μsec after the start of the heating pulse. $\omega_{pe}/\omega_{ce} = 1$ $\omega_o/\omega_{ce} \simeq 1.5$. (b) Energy distribution for different times (t) after the start of the heating pulse; $P_o = 25$W. (After Grek and Porkolab[66]).

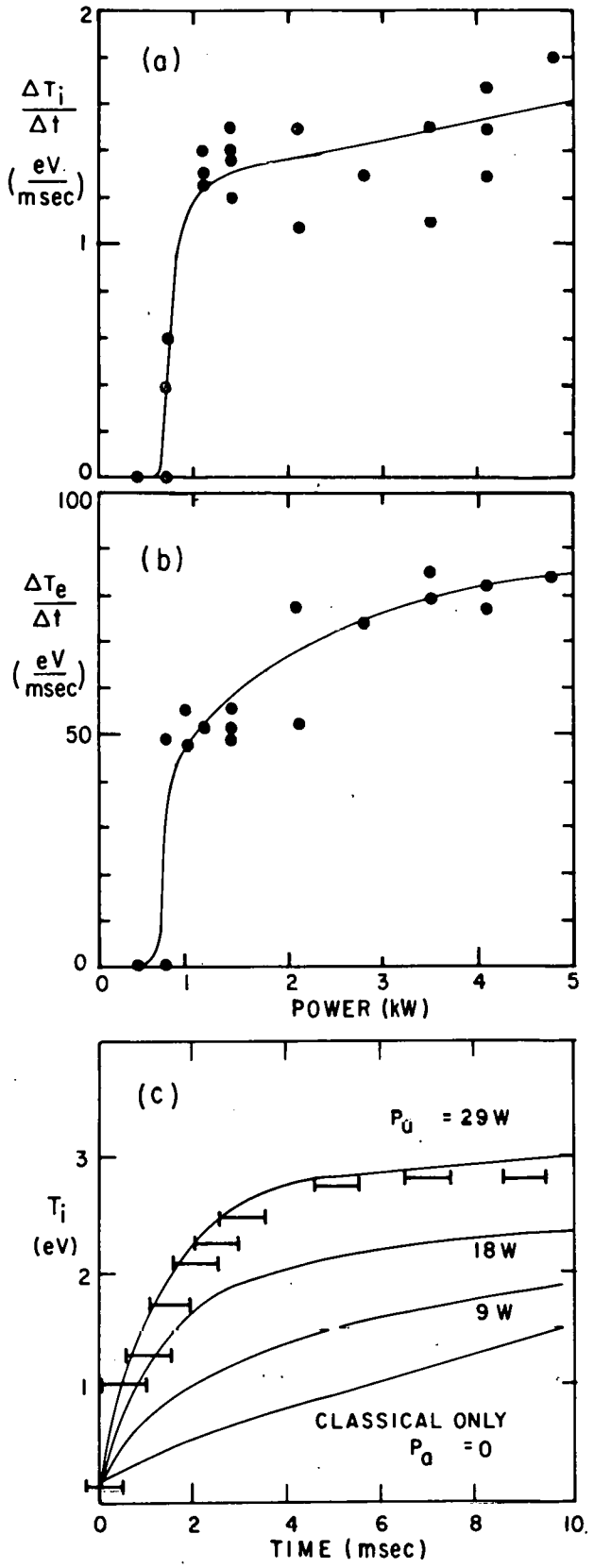

733350

Fig. 10. (a) Heating rate of ion temperature versus input power. (b) Heating rate of electron temperature versus input power. (c) Comparison of time dependence of T_i with numerical calculations. (After Okabayashi et al.[68]).

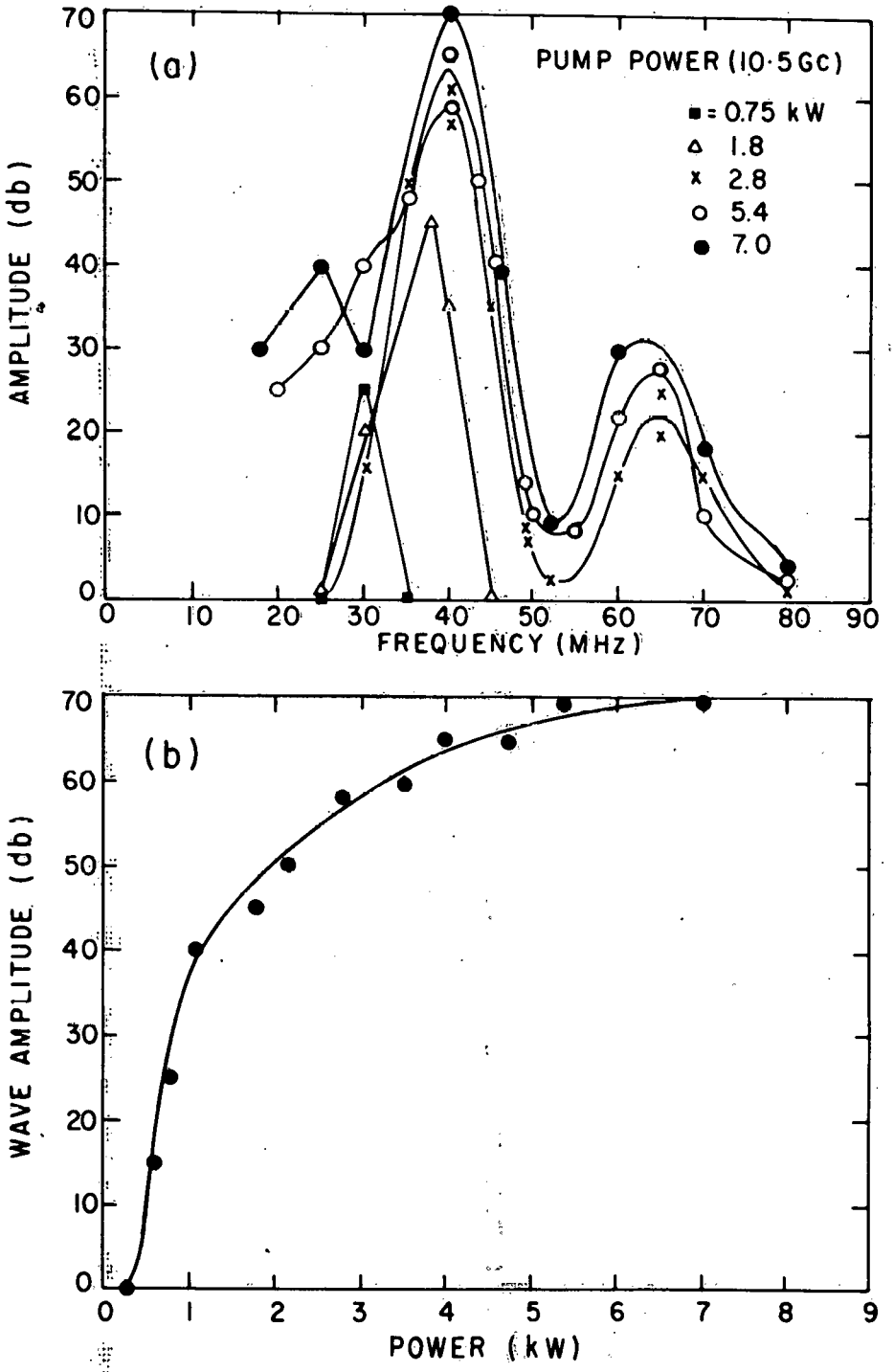

733306

Fig. 11. (a) Frequency spectrum for different input rf powers. (b) Decay wave amplitude versus input power. (After Okabayashi et al.[68]).

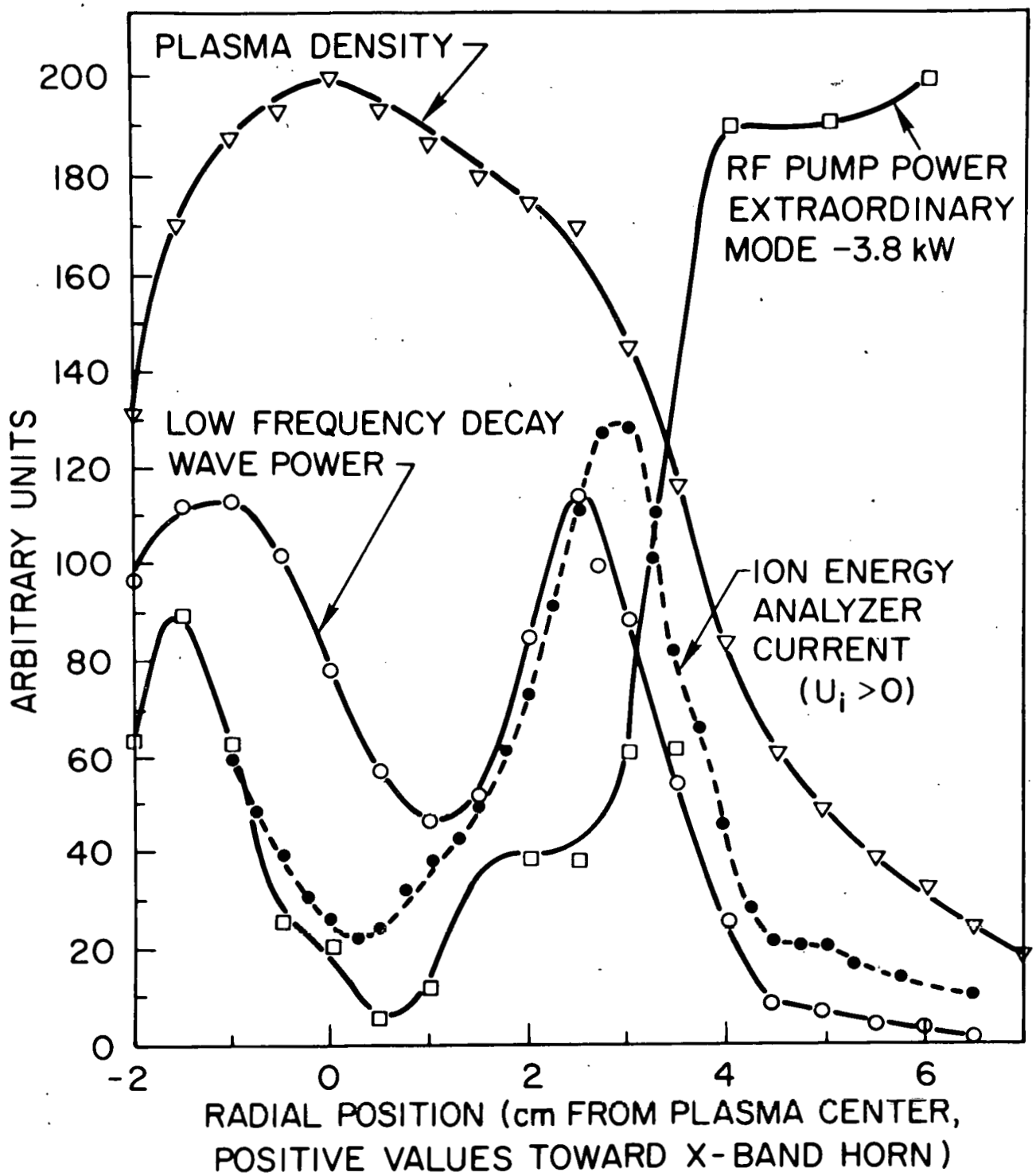

753533

Fig. 12. Localization of decay wave spectrum, ion energy, and relative RF pump power. P_{in}=3800 watts. EO mode. (After Porkolab et al.[67]).

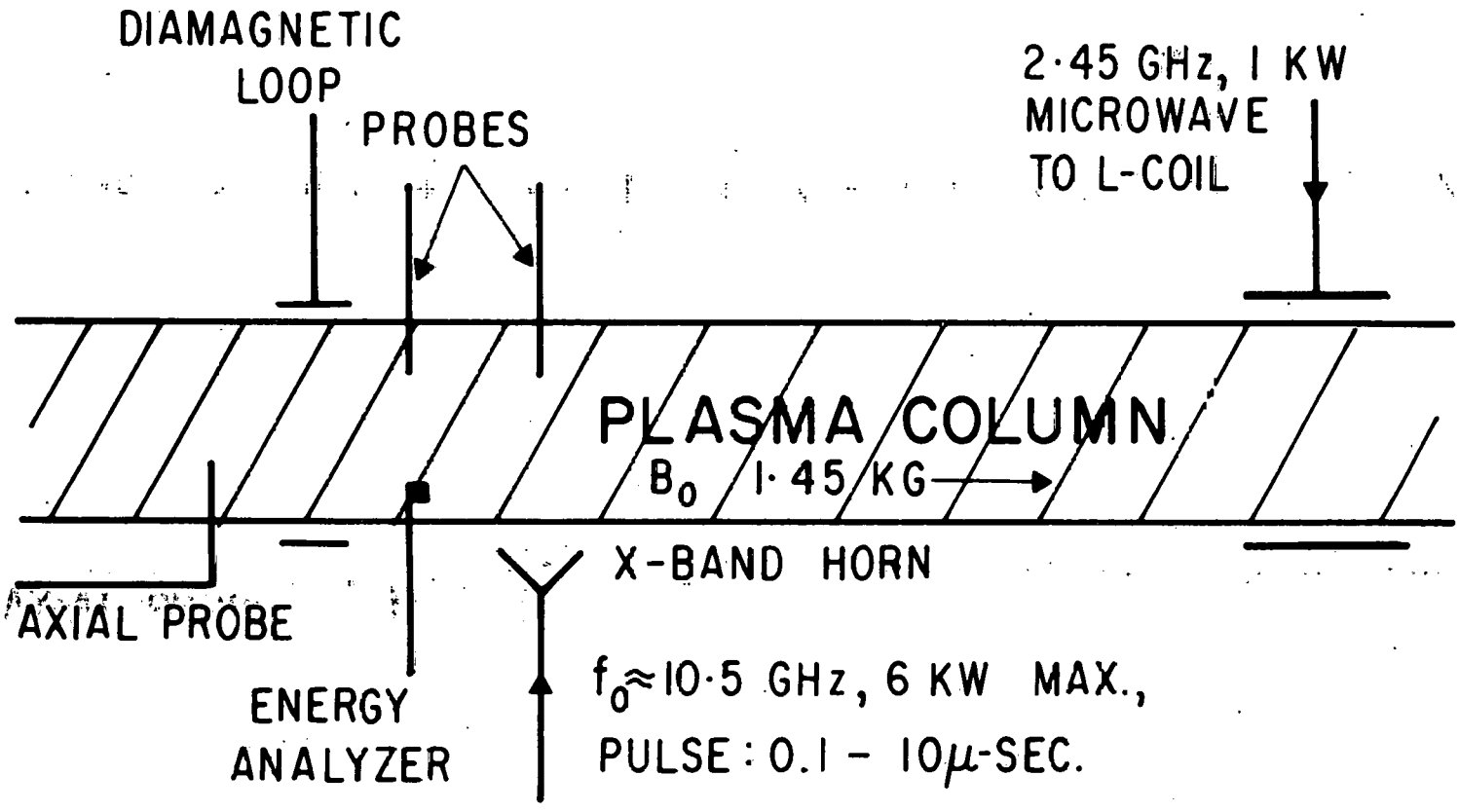

753524

Fig. 13. Experimental setup to measure parametric instabilities in an inhomogeneous plasma. (After Porkolab et al.[67]).

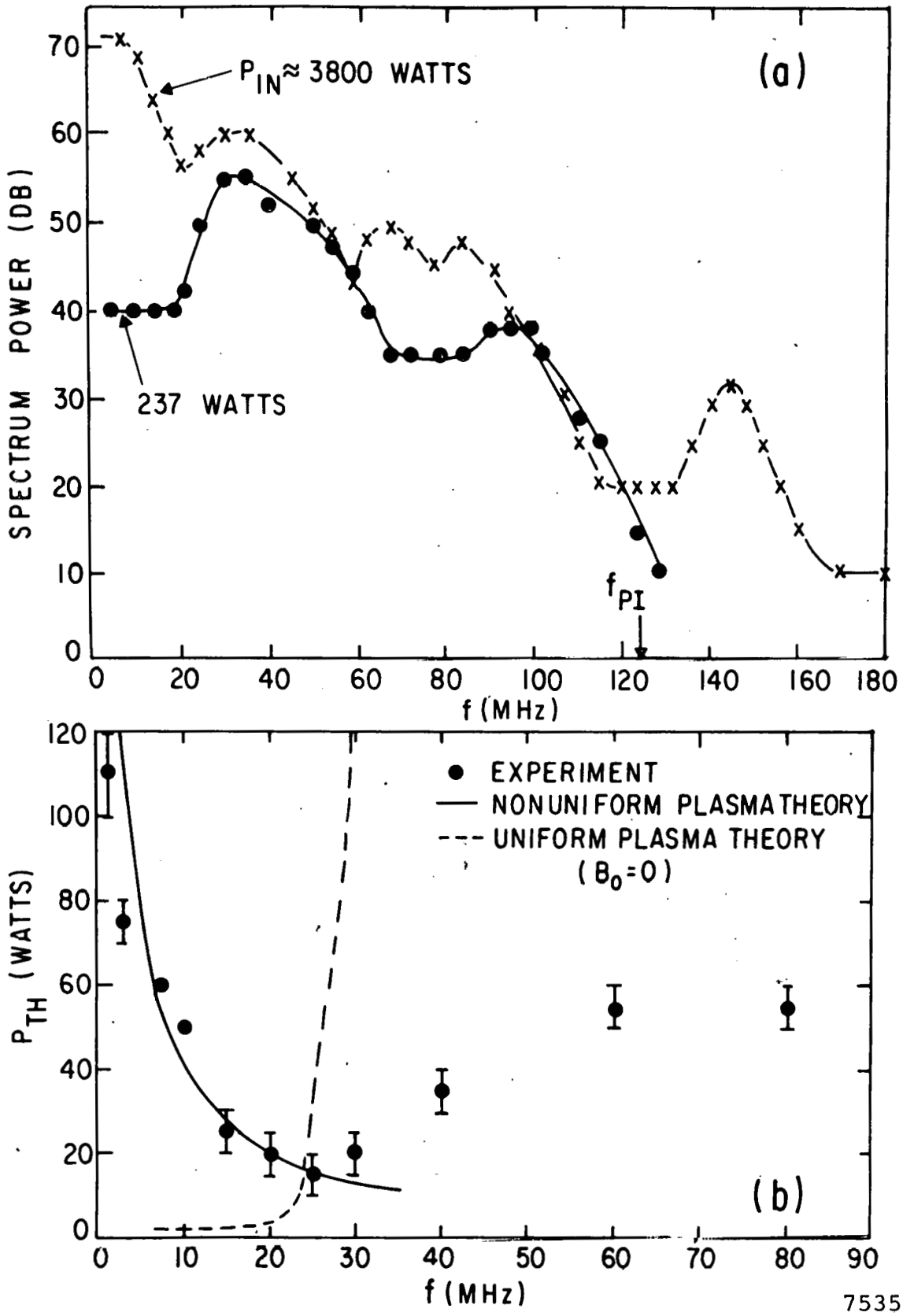

Fig. 14. (a) Low frequency decay spectrum. O-mode (b) Experimentally measured thresholds at A=1 (dots), uniform plasma theory (dashed line), and nonuniform plasma theory (solid line); (the latter calibrated on absolute scale from the incident power levels); O-mode. (After Porkolab et al.[67]).

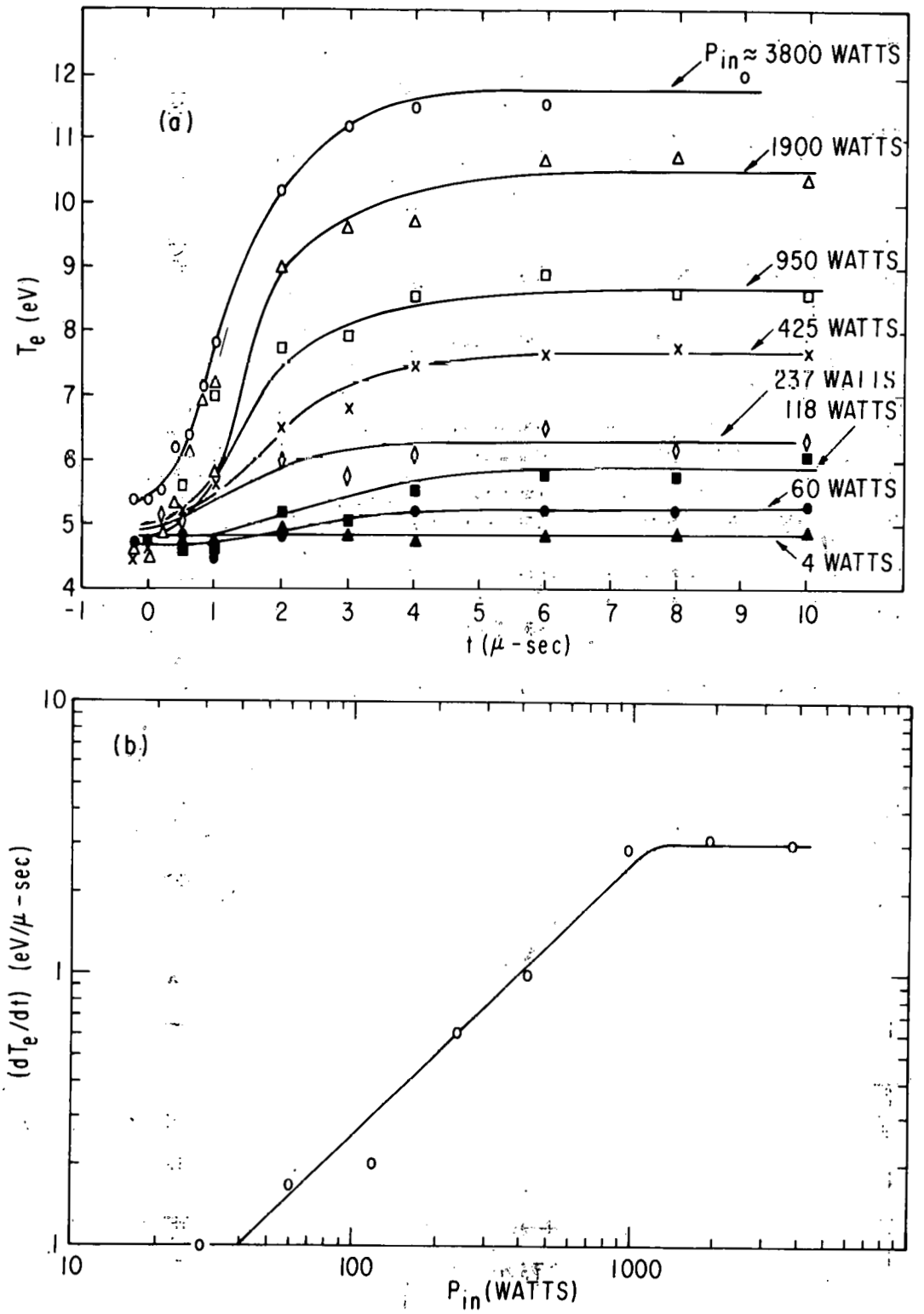

Fig. 15. (a)Temperature obtained from a Langmuir probe as a function of time and input power; O-mode. (b)Initial heating rates in the first few micro-seconds as a function of power; O-mode. (After Porkolab et al.[67]).

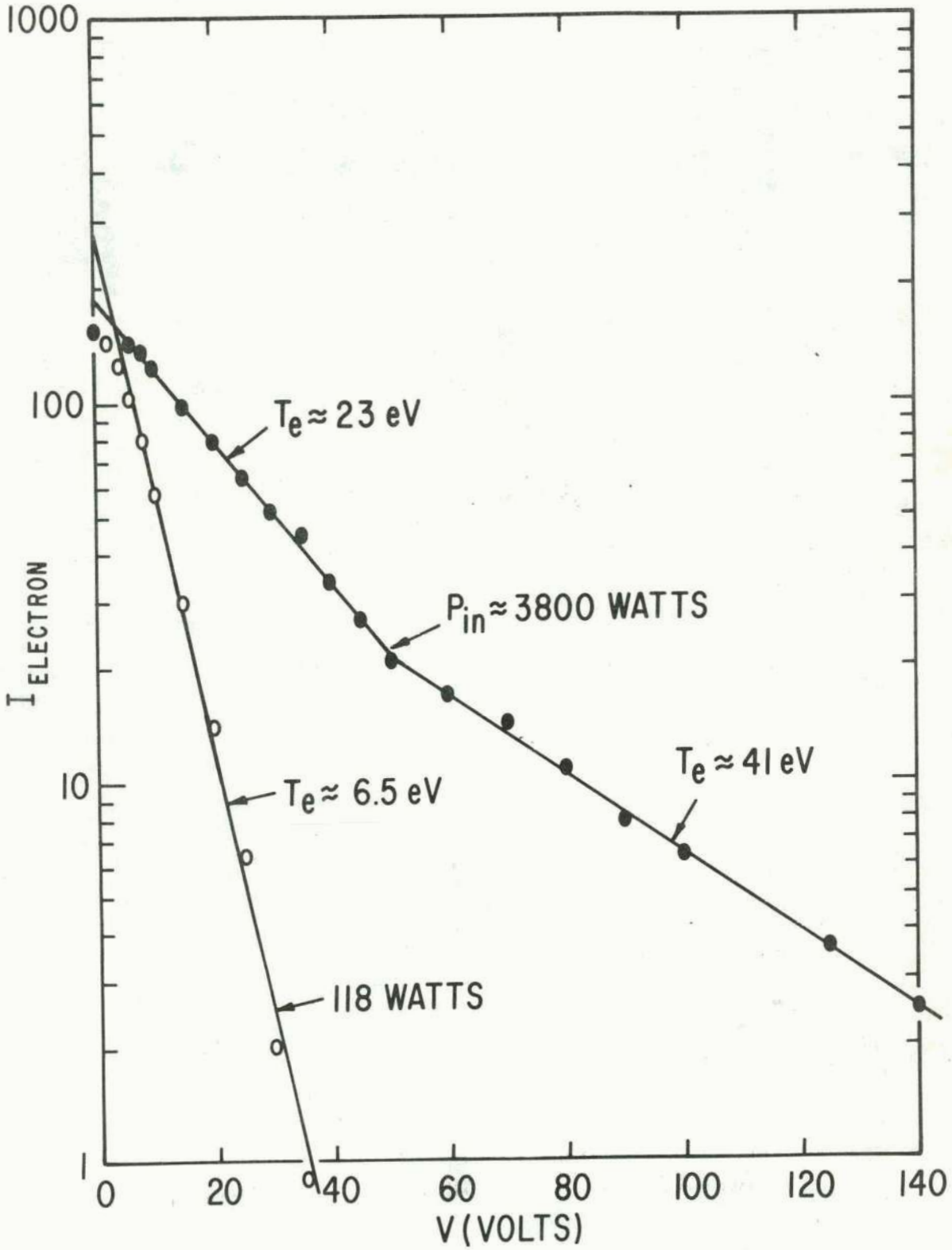

Fig. 16. Energy analyzer measurements of the parallel electron energies; O-mode. (After Porkolab et al.[67]).

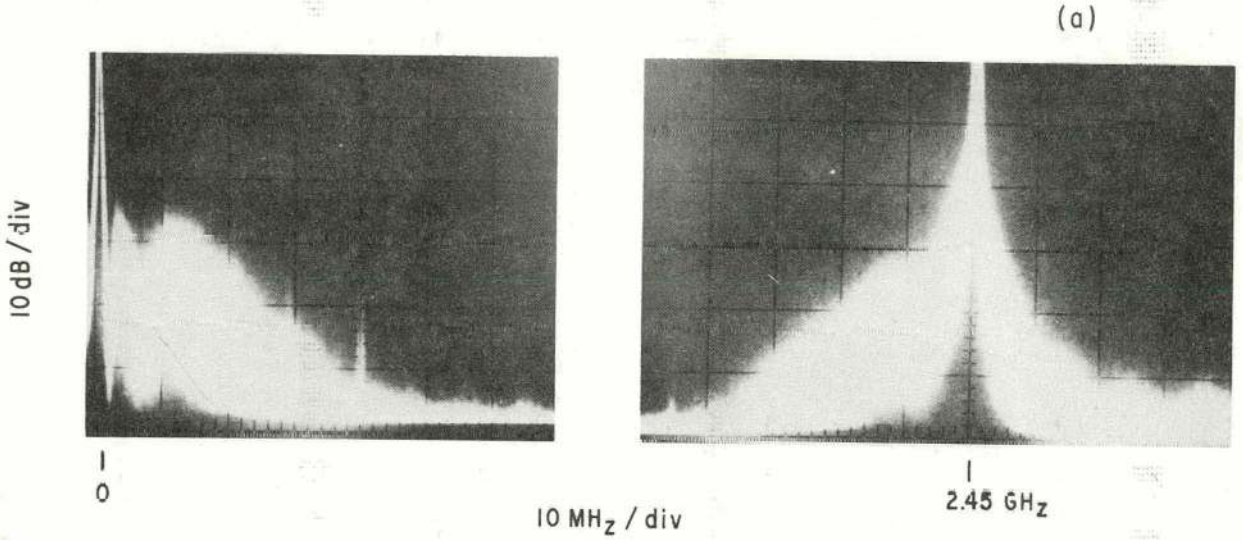

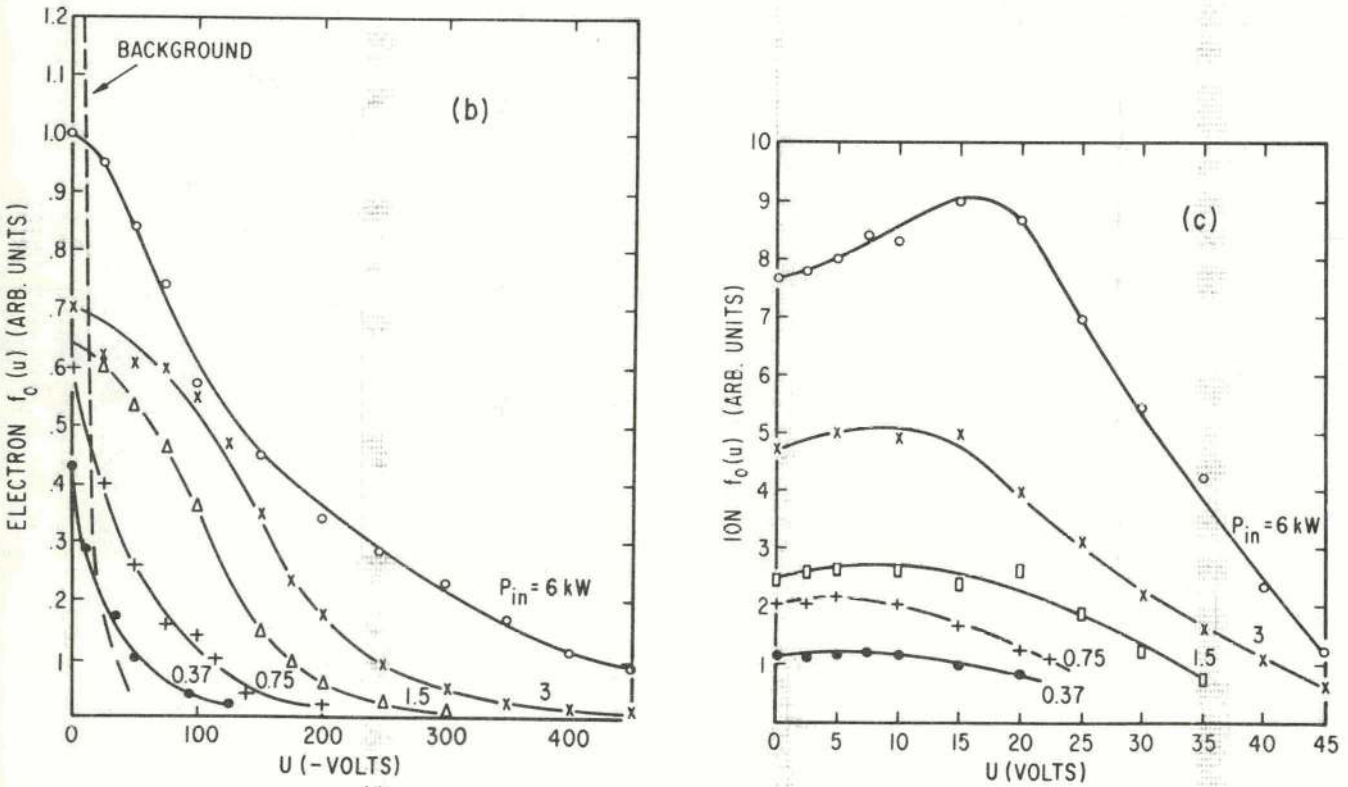

753573

Fig. 17. Decay spectrum (a), and parallel component of the electron distribution function: (b) shows electrons, and (c) shows ions. τ=10 μsec pulse width. ω_o/ω_{pi}=20, ω_{pe}/Ω_e=2 (After Porkolab et al.[71]).

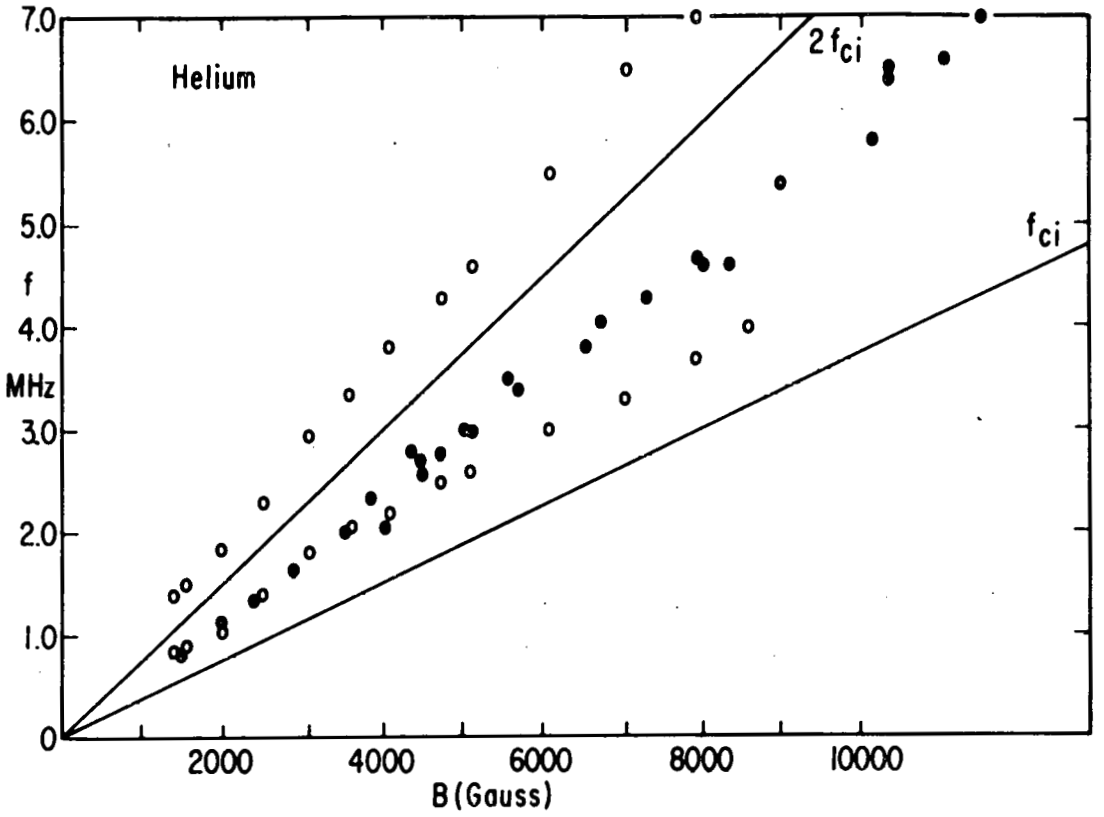

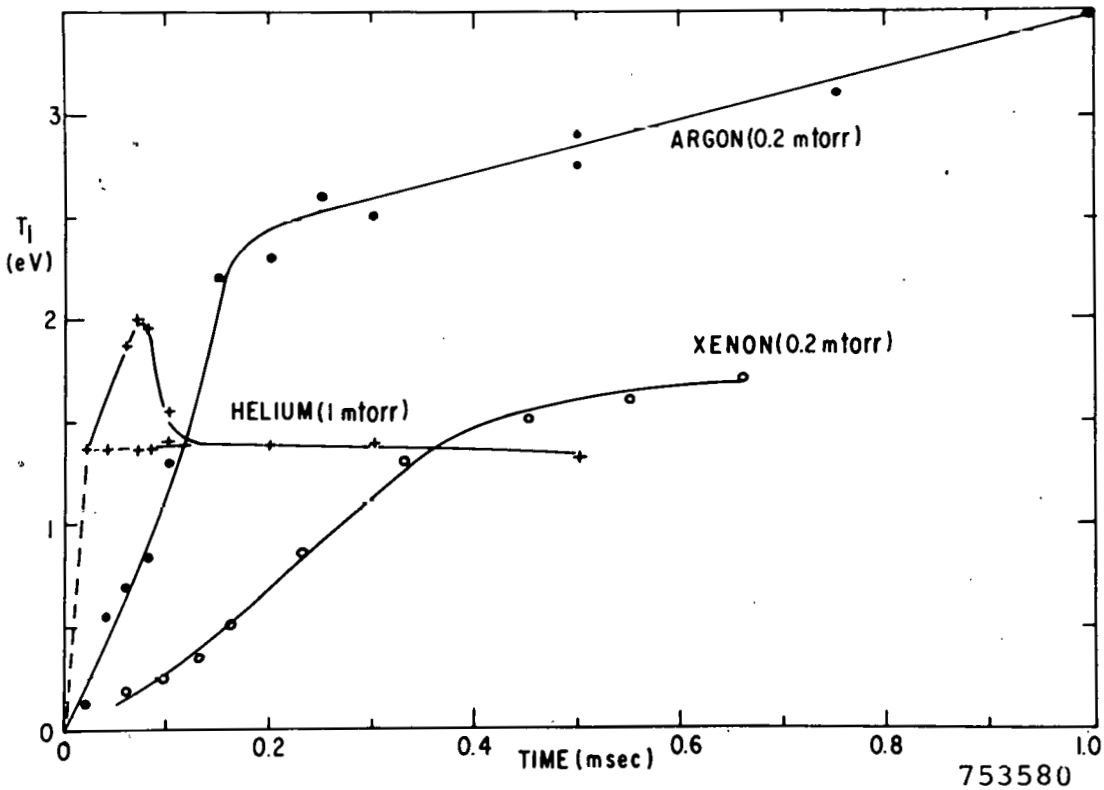

Fig. 18. Low frequency component of the decay spectrum, and ion temperature in different gases as a function of time. $P_{in} \simeq 1.5$ kW, $\omega_{pe}/\Omega_e \simeq 0.3$, $\omega_o/\omega_{pi} \simeq 3$(He), 10(Ar), 15(Xe). (After Bernabei et al.[74]).

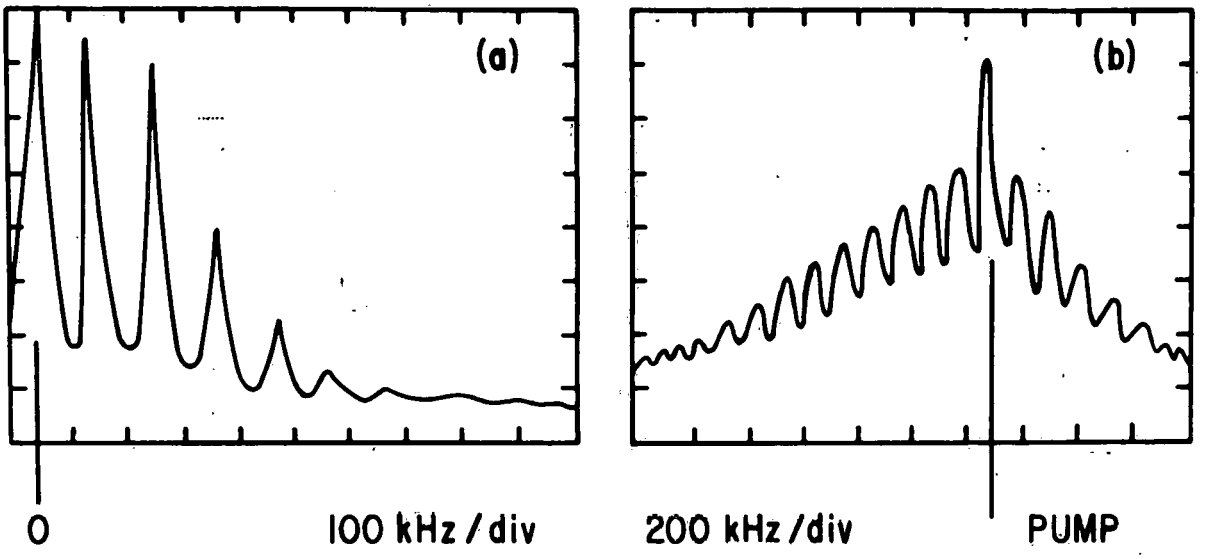

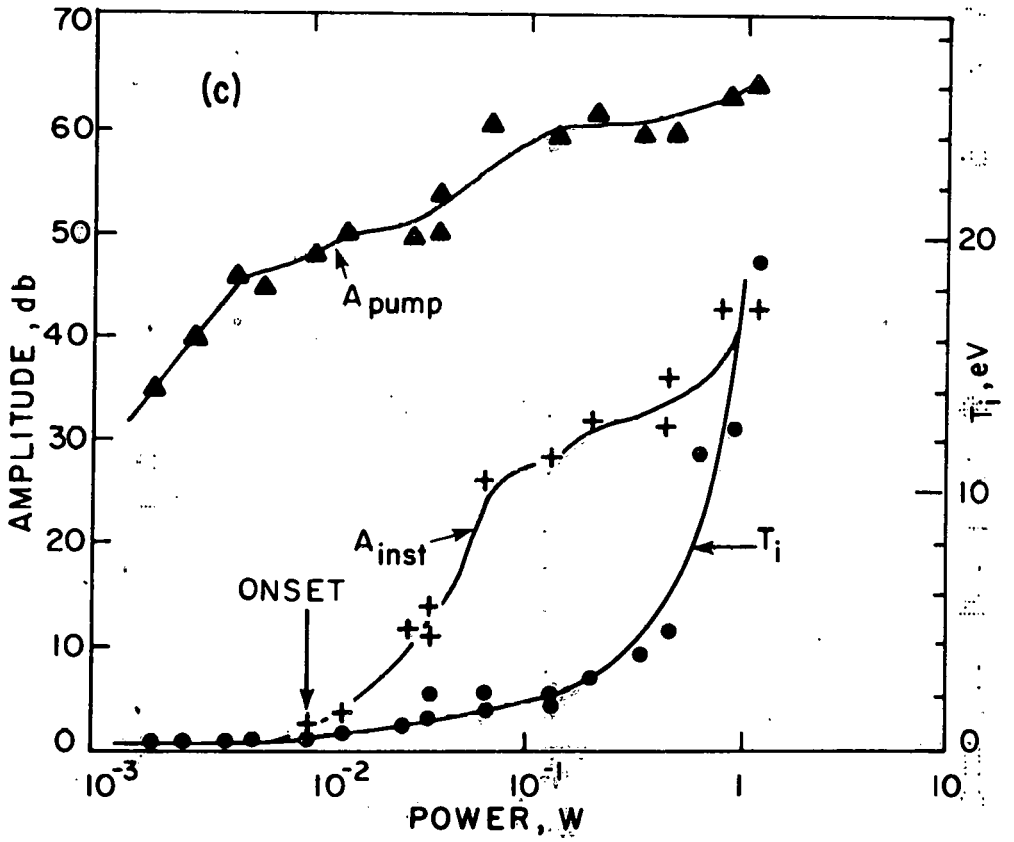

Fig. 19. Low and high frequency decay spectrum, amplitude of the pump and the high frequency decay waves, and the ion temperature as a function of input of power. (After Chu et al.[73]) .

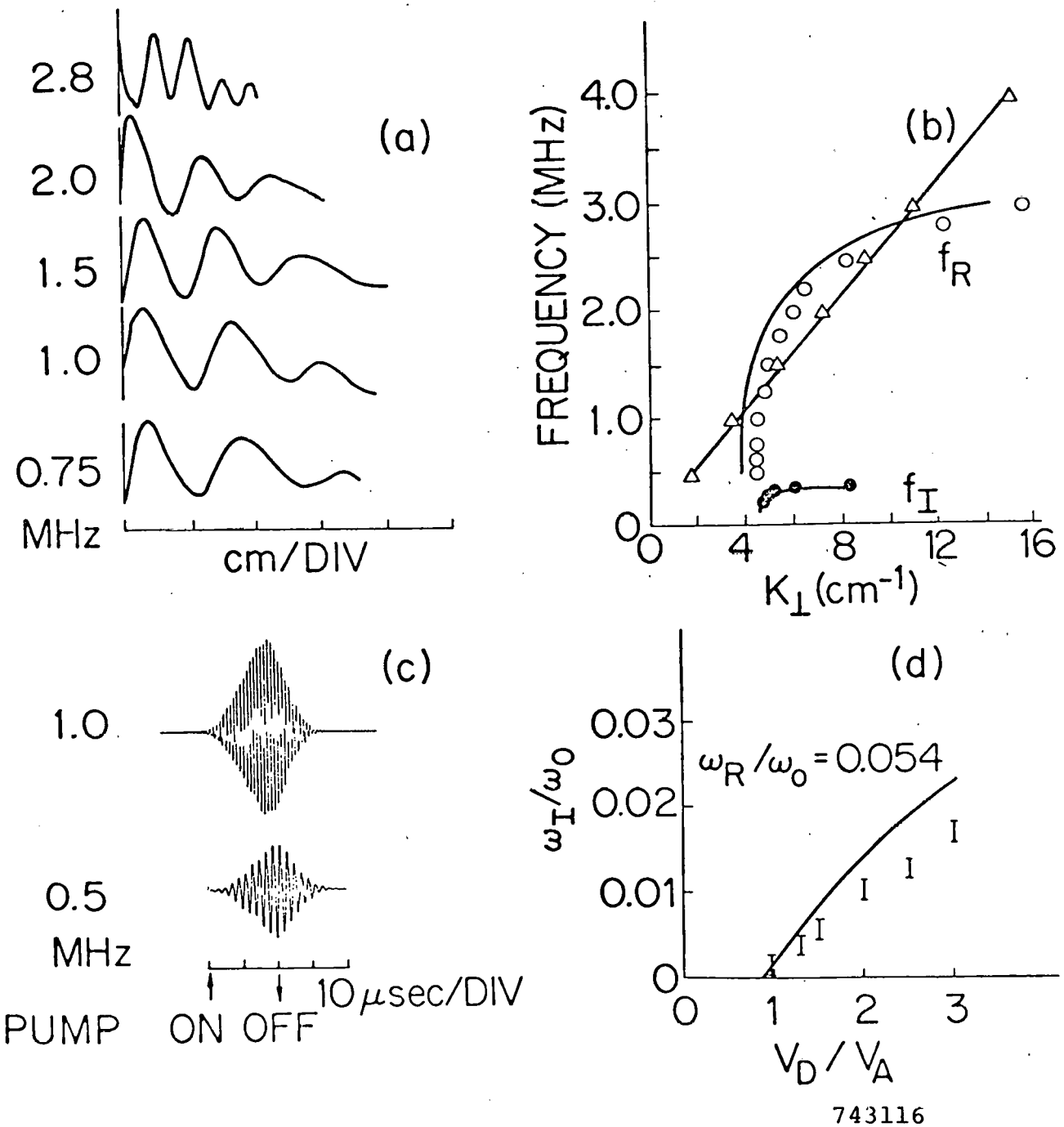

Fig. 20. (a) Interferometer traces of ion quasi-modes propagated at different frequencies. (b) Dispersion curve of the ion quasi-mode (circles and dots) and the ion acoustic mode (triangles); solid curves, theory of Porkolab[10]. (c) Typical ion quasi-mode oscillation amplitudes after switching on the rf pump field. (d) Growth rates as a function of the E×B drift velocity V_D, versus the acoustic speed V_A. Solid curve, theory. (After Chang and Porkolab[78]).

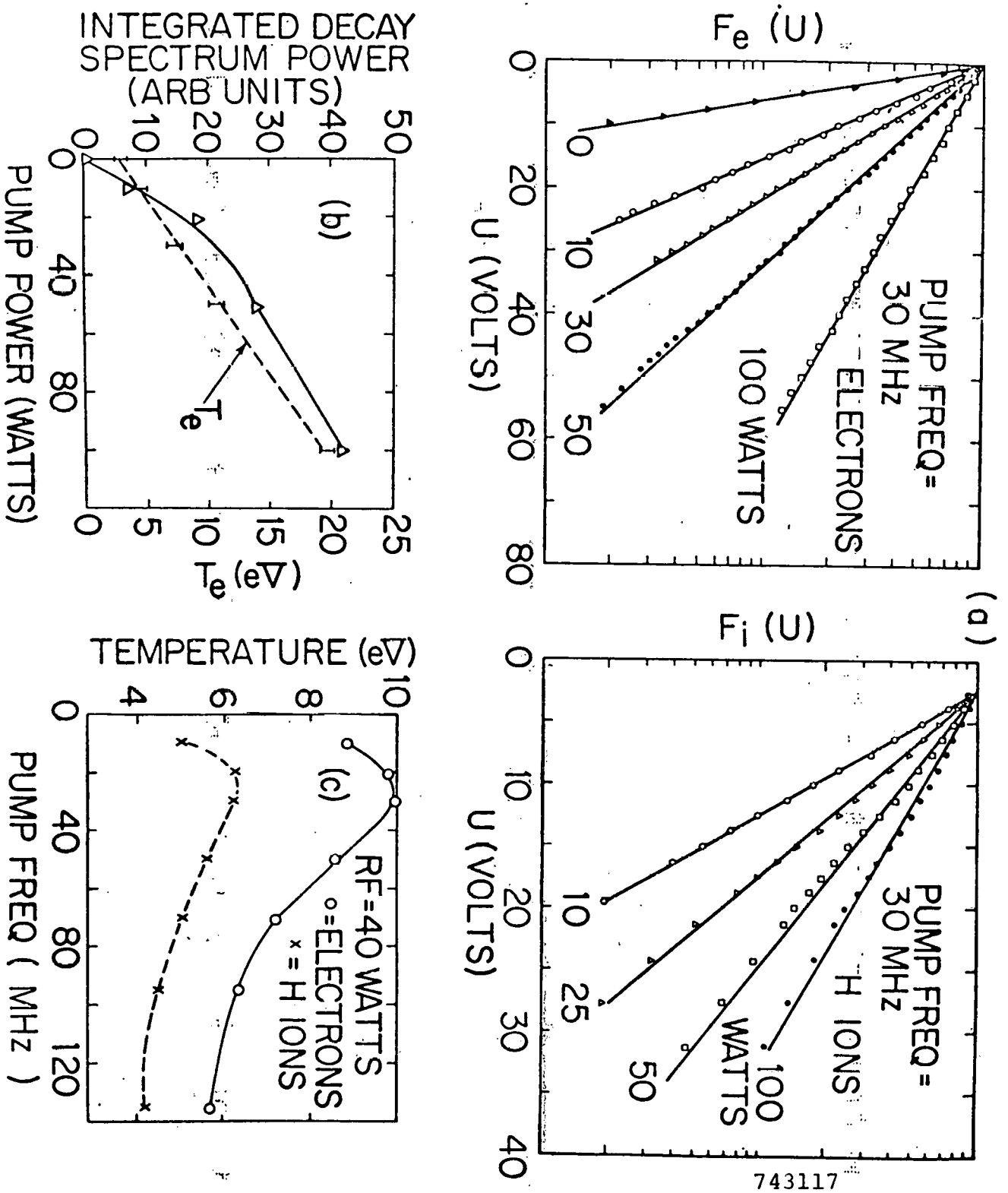

Fig. 21 (a)Electron and ion energy distributions for different rf pump powers. $\omega_o/\omega_{LH} \simeq 1.5$. (b)Integrated decay wave power (triangles) and electron temperature as a function of the pump power. (c) T versus ω_o for fixed pump power; $f_{LH} \simeq 20$ MHz. (After Chang and Porkolab[78]).

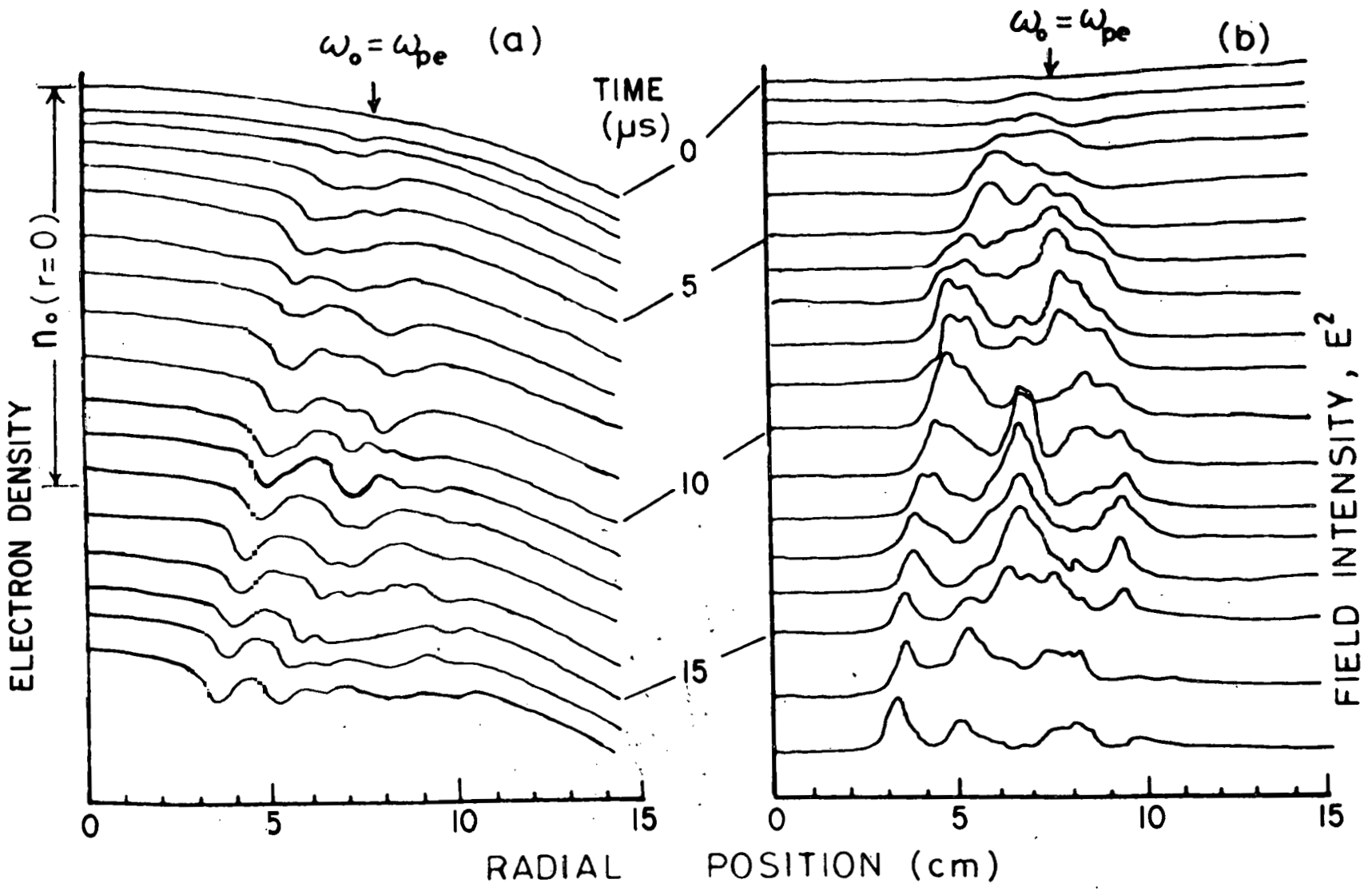

753570

Fig. 22. Profile of the density perturbation (a) and the high-frequency field intensity (b) A stepwise pump starts at t=0. Pump power = 20W. (After Ikezi et al.[102]).

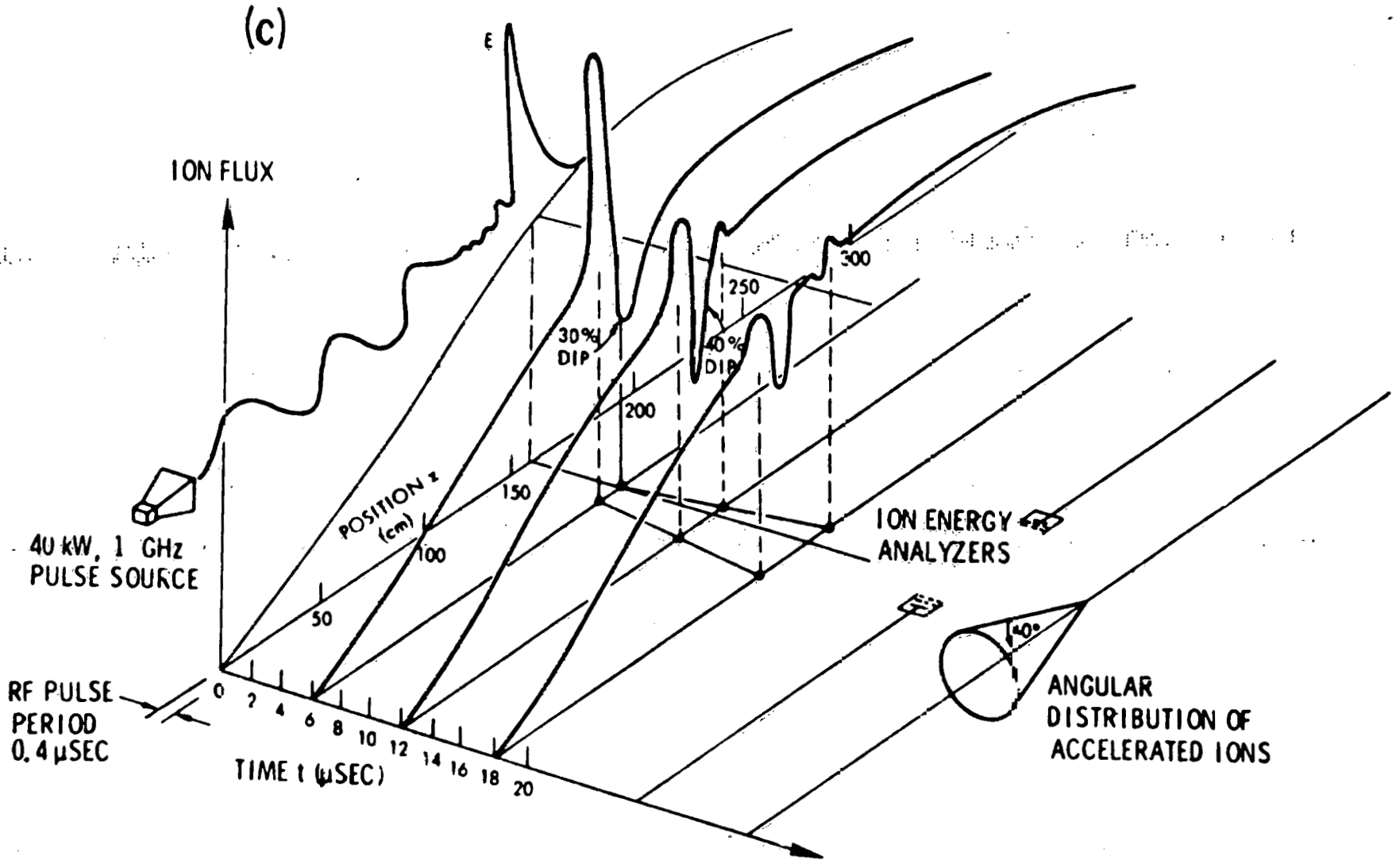

753571

Fig. 22(c). Space-time representation of ion bursts (shaded) driven by the ponderomotive force. Density cavities are created as a result of ion expulsion. The polarization of ion trajectories is represented by the cone with a half-width of 40° with respect to the z axis. (After Wang and Stenzel[103]).